8-2015

Two-dimensional dynamics model of the lower limb to include viscoelastic knee ligaments

Eduardo Granados
University of Texas-Pan American

TWO-DIMENSIONAL DYNAMICS MODEL OF THE LOWER LIMB TO INCLUDE VISCOELASTIC KNEE LIGAMENTS

A Thesis

by

EDUARDO GRANADOS

Submitted to the Graduate School of
The University of Texas-Pan American
In partial fulfillment of the requirements for the degree of

MASTER OF SCIENCE

August 2015

Major Subject: Mechanical Engineering

TWO-DIMENSIONAL DYNAMICS MODEL OF THE LOWER LIMB TO INCLUDE VISCOELASTIC KNEE LIGAMENTS

A Thesis
by
EDUARDO GRANADOS

COMMITTEE MEMBERS

Dr. Dumitru I. Caruntu
Chair of Committee

Dr. Robert Freeman
Committee Member

Dr. Young-Gil Park
Committee Member

August 2015

ABSTRACT

Granados, Eduardo, Two-Dimensional Dynamics Model of the Lower Limb to Include Viscoelastic Knee Ligaments. Master of Science (MS), August, 2015, 89 pp., 6 tables, 41 illustrations, 55 references, 100titles.

A dynamic, 2D, anatomical knee joint model has been developed to simulate knee reactions to external input forces. A deformable contact area approach is used to find contact forces and moments, and a method of applying nonlinear viscoelastic ligament strain rate response was also developed and implemented on the model to account for the effects of viscoelasticity on the ligament fibers. The ligaments were then tested for various deficiencies to identify their effects on the natural frequency of the knee.

Internal knee forces from ligaments, muscles, and contacting surfaces are modeled and then numerically found for different exercises. Static and dynamic equations for knee motion are developed. These equations are then transformed into differential algebraic equation (DAE) systems for modeling various exercises. The DAE systems and the model simulations are performed using Matlab solver ODE15S, and predicted data from the model is compared to data published in literature for validation.

DEDICATION

The completion of my graduate studies would not have been possible without the love and support of my family. My mother, Minerva Granados, always has been supportive and has made my life as easy as she possibly could to help me focus on my studies. My father, Eduardo Granados, Sr., has always worked extremely hard and honestly, showing me by example what it takes to be a good father and a good man. My brothers, Isai and Jose Alberto, have always been there for me when I need them, and my sister, Brenda, helps me out whenever she can. I dedicate this thesis to my family, because they have made it possible for me to pursue my graduate degree in mechanical engineering.

ACKNOWLEDGMENTS

I am very grateful for the guidance and dedication of Dr. Dumitru Caruntu, the chair of my dissertation committee. He has been an outstanding example of professionalism and expertise in his craft, and has given me great knowledge of life, and how to cope with difficult challenges. The numerous times that I have been stuck in a conceptual problem, Dr. Caruntu has been optimistic, helpful, and the ultimate source for knowledge and problem solving ideas. I appreciate this opportunity he has given me and would like to thank him for his dedication to this research.

I would also like to thank Dr. Robert Freeman and Dr. Young-Gil Park for their helpful advice and comments during my defense and seminar presentations. They have given me great feedback and challenged the way I think. For that, I really thank my committee for their help.

TABLE OF CONTENTS

Page

LIST OF TABLES

Page

LIST OF FIGURES

Page

CHAPTER I

INTRODUCTION

1.1 Modeling the Human Knee

Numerically simulating the dynamics of the knee joint is a challenging task. The knee is composed of biomaterials with viscoelastic and nonlinear behavior, in addition to bones with complex surface profile interactions. Two and three-dimensional (2D and 3D) models have been developed in order to predict responses of the knee joint. 3D models include mathematical and finite element formulations. The 3D models, although more accurate, are computationally intensive and require significant time and resources to generate results. For certain exercises, sufficient accuracy can be obtained by using a 2D model. For example, the knee extension is an exercise that can be investigated along the 2D sagittal plane. The sagittal plane passes through the body from front to back, splitting the body into right and left halves [1]. Therefore, for exercises that occur along this 2D plane, such as cruciate ligament deficiency testing of the knee in extension and flexion, a 2D model can be adequate and accurate.

The knee joint is composed of three bones femur, tibia, and patella, articular cartilage, menisci, and four main ligaments. The ligaments of the knee are the anterior cruciate ligament (ACL), posterior cruciate ligament (PCL), the medial cruciate ligament (MCL), lateral cruciate ligament (LCL), and posterior capsule ligaments. For problems in the sagittal plane, the ACL and PCL fibers are the dominant ligaments because their restraining motion is primarily along the sagittal plane [2]. Injuries to the knee joint are amongst the most common in sporting

activities and understanding the anatomy of the joint is fundamental in understanding subsequent pathology.

When researching the behavior of the human knee, one would assume that by now all its mechanics would be fully understood, re-engineered, and numerically replicable. However, due to its unique structure and complexity, the human knee still has a variety of research opportunities. The bones in the knee (femur, tibia, and patella) are held together primarily by four major ligaments and by tendons that are each connected to a bone surface at different areas along the knee and flexor-extensor muscles. As a result, each knee movement produces a unique load in the ligament fibers.

Another difficulty in modeling the knee is that one cannot measure the exact ligament insertion points, bone structure, and cartilage of a live specimen. For ethical reasons and due to the limitations of the current *in vivo* sensor technology*, in vivo* measurement is currently unavailable for ligaments and cartilage. Because of this, an alternative is to develop a mathematical model based on anatomical data from cadavers.

Using a mathematical model, the forces in each ligament and in the cartilage can be estimated at specific levels of knee flexion. These forces cannot be measured from in vivo experiments. This creates many opportunities for research and has potential benefits that could benefit health science.

For example, understanding the internal knee forces at individual positions can be used to benefit rehab patients who have damaged major ligaments, such as ACL or PCL, by allowing rehab specialists to design specific exercises that focus forces on the area of recovery. Another application is in the development of prosthetic knees, which will be able to benefit from ligament specific engineering simulating real knee behavior. At this time, there is still a gap in function

performance between a natural human knee and a prosthetic. As the effects of the insertion locations and the mechanical properties of the ligaments are modeled, highly stable knee joint that can be used to perform highly athletic and rapid response movements at the highest level of sporting competition can be understood.

Another application for a knee model is for the diagnosis of ligament deficiencies. If the knee model can be integrated with motion capture analysis technology, one is able to identify the difference in the response of a ligament deficient knee and a ligament intact knee for different exercises. This data will then be used to determine the condition of ligaments during *in vivo* experiments. In Chapter 5, the model developed in this work is used to compare the behavior of the intact knee with ACL and PCL deficient knees.

Due to the flexible code structure built into this knee model, frequency responses and other forms of non-intrusive ligament deficiency testing can be simulated. The utility of a sagittal plane 2D model is broad, and many other applications for this model are yet to be harnessed.

1.2 Sagittal Plane Model

A 2D dynamic knee model has been developed to simulate the forces and moments in the knee joint induced by static and dynamic loading during knee flexion in the sagittal plane. Deformable contact of the knee is used to model the articular cartilage, and viscoelastic ligaments are implemented to closely simulate ligament mechanical properties.

The human knee is the most complex joint of the human body, and is restrained by 4 ligaments and posterior capsule that are modeled as 10 ligament fibers [3]. In the 2D dynamic knee model, these ligament fibers are pin connected at insertion points on the bones that were found using anatomical data from previous studies [4-7]. Bones of the knee joint are the femur,

tibia, and patella. The articular curves of the bones are each modeled using a 10th degree polynomial fit acquired from digitized cadavers, to approximately match the shape and size of real skeletal bone. The articular curve of the patella was fitted using the Matlab *Grab-It* function from the Matlab Exchange on a patella from a knee *x*-ray. The curves were fitted with 10^{th} degree polynomials.

The knee is classified as a synovial hinge joint with the ability to move in flexion and extension. From fully extended, to deeply bent, the knee has a range of flexion of 135 degrees [8]. In the sagittal plane 2D model, the cruciate ligaments are very important ligaments because they stabilize the knee in the anterior and posterior directions. Therefore, the insertion points of the cruciate ligaments are very important.

The knee modeling is split into different sections in order to give the model more flexibility for adaptation to different problems. The hierarchy of the model makes the solid structures of the knee (the bones) the foundation, and kinematic reference bodies, for the dynamic knee model in Matlab. The model has a section titled "Bones" which sums all contributing forces and moments from ligaments, contact, and gravity about the bone center of mass. This method of development is ideal for the knee model because once the *X*-*Y* coordinate global position of each bone is provided, then separate bone functions calculate the resultant forces and moments about the center of mass. As a result, these bone functions can be readily used by a solver, which will take the important output variables from the functions, and find a solution. In the following chapters, the model theory and development is described in more detail, and the anatomical foundations of the model are also described.

1.3 Anatomical Terms

Several anatomy terms that may be unfamiliar to engineers are used in describing the model. When describing the location of a bone, distal means remote from the point of attachment or origin. Proximal is the antonym of distal and means "closer to the point of observation or attachment." Anterior movement is "forward movement". Posterior is the opposite of anterior and means "toward the rear of an object." Lateral is to the side, and in this case it means further from the midline of the body. So the outer side of the right knee is the lateral side. Medial is the opposite of lateral because it means "closer to the midline." Therefore, the medial sides of the knee are the ends of the knee joint that can touch when a person stands straight up with their feet together [1]. This model is a sagittal plane model, which is an imaginary vertical plane from front to back.

CHAPTER II

ANATOMY OF KNEE JOINT

2.1 Anatomy of Knee Joint

An in-depth understanding of the anatomy of the knee joint is essential to the formulation of any type of knee model. This section will discuss the basic anatomy of the knee joint, and the different techniques used to obtain the data used in the anatomical knee model. It is important to know that the knee is the most investigated joint in the human body, and is the most heavily loaded joint with the highest incidence of osteoarthritis and injuries.

In this model, femur, tibia, and patella are included as the knee joint bones. Fibula is not considered to be a part of the knee joint in this analysis because it does not have any relative motion with respect to tibia. The patella exhibits load bearing depending on the exercise and serves as a lever for the quadriceps and the patellar tendon connection.

2.2 Components of the Knee

2.2.1 Femur

The femur is the largest bone in the human body and is, by most measures, the strongest bone. At its proximal end, the femur is connected to the pelvis (hip joint). Distally, the femur connects to the knee joint. In knee joint motion, the femur slides and rolls along the tibial plateau. The knee articular characteristics are given by cartilage, synovial fluid, and menisci. In

addition, the femur comes into contact with the patella during exercises and is the lever arm that promotes actuation of the lower limb by the quadriceps muscle.

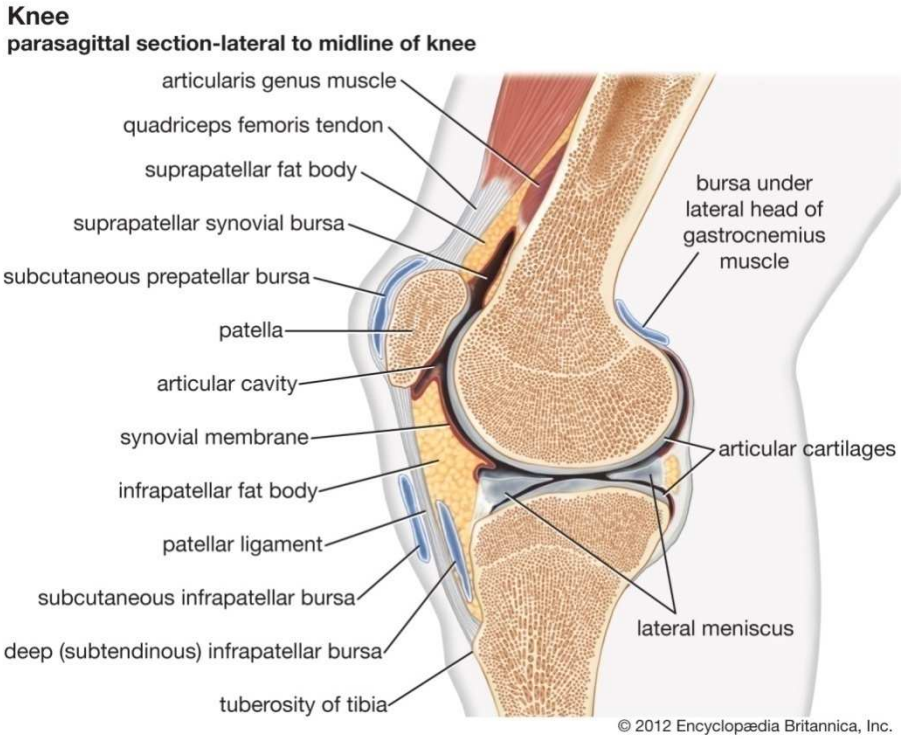

Figure 1: *Anatomy of Knee in Sagittal Plane*

2.2.2 Tibia

The tibia is the bone that connects the knee and ankle joints. It is located next to the fibula in the lower leg and is the second largest bone in the body after the femur. The proximal extremity of the tibia has medial and lateral plateaus. The tibial plateaus and the femoral condyles form the tibio-femoral joint, which is the weight bearing part of the knee joint.

2.2.3 Patella

The patella is a flat triangular shaped bone that is located in the front of the knee. The quadriceps femoris muscle has its tendon insertion point on the proximal apex of the patella. The

biomechanical role of patella is to provide mechanical leverage to the quadriceps muscle [9], which is the extensor muscle of the knee. The distal end of the patella has the insertion of the patellar tendon, which is a ligament connecting the patella to the tibia, and provides extension of the lower leg at the knee joint.

2.3 Ligaments

Ligaments connect tibia and femur and provide stability to the knee. They restrain the tibia and femur to a certain range of motion. They are viscous structures bearing tensile forces. There are four primary ligaments and posterior capsule in the knee [3]. They are the ACL, PCL, MCL, LCL, and posterior capsule. These ligaments are modeled using ligament fibers (fibers). The number of fibers can vary depending on how the 2D model is representing the ligaments, which are 3D structures.

2.3.1 Anterior Cruciate Ligament

The ACL is the ligament that connects the distal-posterior end of the femur to the proximal-anterior tibial plateau. It has two fibers, which are the antero-medial and the postero-lateral fibers, with the antero-medial fiber being connected closer to the anterior side of the tibial plateau. In terms of forces, the anterior fiber has been shown to have slightly higher stress than the posterior fiber in material tests [10].The ACL resists forces pushing the tibia in anterior translation and medial rotation in relation to the femur.

2.3.2 Posterior Cruciate Ligament

The PCL is the counter ligament to the ACL. It connects the posterior end of the tibia plateau to the medial condyle of the femur. This ligament is therefore able to resist posterior tibial movements relative to the femur. It is modeled as two fibers; PCL anterior and PCL

posterior. PCL anterior is stronger than PCL posterior based on material testing. The stress-strain response for the PCL fibers reveals that the ACL fibers are materially stronger than the PCL fibers according to Ref. [10].

2.3.3 Medial Collateral Ligament.

The MCL is located on the medial (inner) side of the knee connecting the femur and tibia. The MCL [11] resists forces pushing the knee medially. Its deficiency leads to low support in countering forces making the knees bend inward toward each other. MCL also has a contribution in the sagittal plane motions. The MCL is modeled as 3 fibers, the MCL anterior (superficial), the deep MCL, and the oblique MCL. The deep MCL is hidden underneath the superficial MCL fibers.

2.3.4 Lateral Collateral Ligament

The LCL is located on the opposite side of the knee as the MCL. It is attached from the top part of the fibula to the lateral epicondyle of the femur and resists lateral movement of the tibia relative to the femur [11, 12]. It also has a contribution in the sagittal plane motions. Unlike the MCL, the LCL is fused with neither the capsular ligament nor the lateral meniscus. This makes it more flexible and less susceptible to injury than the MCL.

2.4 Cartilage and Meniscus

The bones of the knee are not meant to be in direct physical contact with each other. In between the contacting bones there is cartilage that lines the surface of the tibial plateau, femur, and the patellar bone posterior surfaces. Knee cartilage is classified into two different kinds of cartilage. There is fibrous cartilage (articular cartilage), which is what is found on the surface of the bones for shock absorbance, and hyaline cartilage, whose purpose is load distribution

throughout the contacting surfaces. Both will be discussed in further detail in the cartilage modeling section.

2.5 Synovial Capsule

The synovial capsule is a chamber that surrounds the knee and contains synovial fluid. Synovial fluid is a non-Newtonian fluid that behaves differently depending on the strain rate. For example, if an impulsive load is placed on the knee, the synovial fluid would act stiff and dampen the shock, while at slower strain rates it acts similarly to a low viscosity fluid. Additionally, synovial fluid has an extremely low friction coefficient and can therefore be modeled assuming negligible friction [13].

2.6 Quadriceps Muscle

The quadriceps muscle group is connected to patella through the quadriceps tendon. The muscle group is composed of four primary muscles: rectus femoris, vastus lateralis, vastus medialis, and vastus intermedius. The rectus femoris occupies the middle of the thigh and for the most part covering the other quadriceps muscles. It connects patella and pelvis. The three other muscles are between patella and femur and are named according to their position. The vastus lateralis is on the lateral side of the femur. The vastus medialis is on the medial part of the femur (the inner thigh), and the vastus intermedius lies between the vastus lateralis and vastus medialis on the front of the femur. These four major quadriceps muscles can be treated as one unit for most models [9].

When considering the effect on the model, the quadriceps muscle, which is the extensor muscle of the knee, actuates patella. The patella, in turn, acts as a lever for the quadriceps force

and actuates the tibia into a motion of extension. The quadriceps tendon force is due to quadriceps muscle contraction. At certain angles "wrapping" of the quadriceps tendon on the femoral surface occurs [5]. In conclusion, the quadriceps muscle actuates the leg into and extension motion. It has been included in the model in order to perform the knee extension exercise.

CHAPTER III

LITERATURE REVIEW

3.1 Background

In previous studies, various representations of the knee ligament structure have been used. A one-dimensional representation of the knee ligaments was initially used in Ref. [14]. The one-dimensional model was useful when it came to predicting joint kinematics, but was too simple for detailed knee experimentation. Abdel-Rahman and Hefzy later created an anatomical model of the human knee to experiment additional biomechanical behaviors [4, 15]. Their model limited the components of the knee to specific ligament fibers and surfaces for simplification. Bendjaballah et al. [16] related a nonlinear finite element model of the entire human knee joint to better investigate the biomechanics under certain forces. In this case he only considered compressive loads, and the ligaments were modeled as nonlinear springs. Li [17] investigated the knee joint, but considered joint contact stresses. He also modeled the ligaments as nonlinear springs similar to various other models such as Caruntu and Hefzy's [5-7].

Mathematical knee models can generally be classified into two types: anatomically based models, and phenomenological based models [18]. Phenomenological models are general models that take the part as a hole, so the analysis is done on the entire body and the interest is on the overall response of the object. Anatomically based models look at individual components of the structure, so the accuracy of the model is of importance. The 2D dynamic knee model of this work falls under the category of an anatomical model.

3.2 General Knee Models

The knee joint was modeled in terms of a 2D motion analysis of a four bar mechanism [19]. The knee joint is an irreducible joint because each of its four complex parts in the linkage model needs to exist simultaneously and in a complex assembly to be able to perform its basic function. The two bones perform the rolling and sliding motion and the two cruciate ligaments act as mechanical links and perform a vital guiding function in the joint. The cruciate ligaments form the two crossed bars whilst the upper and lower bones effectively form the other two bars. In a four-bar hinge, the length of each of the four bars remains constant, but the angle between each bar can change so the lower leg can rotate. An important feature of the four-bar hinge is that the instantaneous center of rotation approximately coincides with the crossover point of the cruciate ligaments. This crossover point moves as the joint opens and closes so that the knee does not have a fixed point of rotation, as does a simple pivot joint. Results from this study found that this simple 2D model could be fairly accurate in predicting forces in the ACL and PCL.

Other 2D Models are anatomical which provides a more accurate representation of the knee [18]. Such models include ligaments, contact, and muscle forces as contributors to the knee mechanics. With this in mind, several components of the 2D models found in published literature, such as other ligament and cartilage models will be discussed next.

As mentioned before, ligaments are used biomechanically to stabilize the knee and are essential to maintain good posture. The four ligaments that are in the knee are ACL, PCL, MCL, and LCL. The way they are usually modeled in the two dimensional sagittal plane is as 10-12 ligament fibers that compose the 4 ligaments. For example, the ACL has 2 components (fibers) in the models: ACL anterior and ACL posterior. These fibers, having 2 insertion points on femur and 2 on tibia, better describe the ligament's behavior [3].

The ligament biomaterial is viscoelastic [20]. Testing of the elastic behavior has revealed that ligaments have a non-linear stress-strain (force-length) relationship. Ligament elastic behavior is described by a non-linear (quadratic) force-strain relationship, followed by a linear relationship after a strain threshold has been reached [21]. The ligaments forces are modeled like nonlinear springs. Ligaments are a significant contributor to knee stability. Therefore, their insertion points on the bones are critical in knee models. The positions of the ligaments need to be as accurate as possible.

The insertion points for the ligaments and the anatomical curves used to model the bones have been well documented in previous investigations [3, 4, 22]. The means to obtain this data has been to use the cadavers for investigations of their ligaments and knee structure [17, 23]. The positions of the ligaments, bone *x*-rays, and 3D mapping have been unified to generalize this data in models. Knee ligaments are unique to each individual in material characteristics, size, and insertion point locations.

The locations of insertion points have been reported in several papers, more recently [24]. Several doctors aimed to improve the location of the ACL that is currently used in surgeries to decrease the likelihood of making a mistake during an operation. The doctors found an improved location for the tibial insertions of the ACL and suggest that now surgeons can be more accurate in correcting a torn ACL. These types of landmark experiments are ongoing and will help increase the accuracy of models that are being created.

3.3 Cartilage and Meniscus

The knee joint is a pivotal hinge joint that controls the flexion and extension movement of the lower leg. When these movements are performed, the bones of the joint, the femur and

tibia, rub and roll against each other. Bone on bone contact can be very painful; exhibited by people who suffer from cartilage damage and osteoarthritis. Cartilage layers cover the surface of the femur and the surface of the tibial plateau where rolling occurs, thus preventing the bones from direct contact while also reducing friction. The meniscus is also in between tibia and femur and distributes the joint load to a broader area of the bones. The meniscus refers to two parts of the knee, the lateral and medial menisci. These two menisci provide structural integrity to the knee when it undergoes tension and torsion [22]. Removal of the menisci [25] revealed higher contact stresses along with smaller contact area.

Another important property of the knee that makes it special is that it is a synovial joint. A synovial joint is an encapsulated joint containing synovial fluid. The synovial fluid is a low friction lubricant that exhibits non-Newtonian behavior [26]. The synovial fluid in the knee seeps into the cartilage pores and is able to increase the shock dampening qualities of the articular cartilage in the knee. It does so by a system of weeping lubrication, which is a surface lubrication method that works under applied pressure. Weeping lubrication is when a sponge-like layer is compressed, resulting in the excretion of a fluid embedded within the layer. In the case of the knee cartilage, when the knee is under a compressive load, synovial fluid reserves in the cartilage are slowly squeezed out, providing more lubrication when it is needed most. Additionally, the synovial fluid exhibits a change in viscosity at higher applied stresses. Therefore, when the compression is high, the synovial fluid thickens to dampen the shock, and when the pressure is released, it resumes its lubricating functions. Another name for this type of fluid is a dilatant (or a shear thickening) material [27]. Synovial fluid is an excellent lubricant. Therefore, frictional effects on the knee can be neglected in models [13]. For synovial fluid the friction coefficient μ is between 0.005 and 0.02.

3.4 Dynamic Effects on Cartilage

A healthy knee represents the optimal biomechanical structure for the joint, but what happens when the cartilage in the knee becomes damaged? Many studies have tried to analyze the mechanisms for failure of cartilage. Additionally, several studies focus on the dynamics of the knee joint and how external forces affect the cartilage.

One such study undergoes a series of tests to test the hypothesis that knee joint pain may be caused by our neuromuscular control of limb motions [28]. Data accumulated from 18 patients with knee pain and 14 patients without knee pain was analyzed. The patients were told to walk naturally past a walkway that had a six component force plate, with EMG's and accelerometers on, all while under the observation of a three camera, 200Hz Vicon motion-analysis camera system. All patients (with and without knee pain) exhibited similar knee cadence, ground reaction forces (GRF), and walking speeds. However, where there was a distinct and statistically significant difference between the two groups was in the analysis of the GRF versus time during the walking cycle. The patients with knee pain happened to have a shorter time span between the heel impact and the GRF, showing a correlation between a greater impulse at heel strike and knee pain. Not only was it discovered that for the group with knee pains the loading rate of the ground reaction force was higher, but also that the landing of the ankle had a larger downward velocity, which was accompanied by a larger angular velocity of the shank. The rapid upsurge of the vertical GRF pushed the shank into hyperextension at the knee, causing a more violent follow-through when walking. In animal testing, it has been repeatedly shown that impulsive loading consistently provokes osteoarthritis, and this study shows that the manner in which people walk, based on their neuromuscular control, can lead to osteoarthritis in their joints. The conclusion that can be drawn from this research is that

impulsive loading on the cartilage has deleterious effects that can ultimately lead to osteoarthritis [29]. Walking in a smooth, rolling manner is a suggested way of preventing cartilage damage.

3.5 Cartilage Models

Contact forces in the knee models are calculated using a variety of methods depending on the model being used. One such method found in 2D models is the use of the normal vectors of the contact curves to calculate the contact force [4, 23]. As one progresses point-by-point along the tibial and femoral curves of the knee joint, the vectors normal to each curve are found. At only one position for the contacting curves, there will be a set of normal vectors for the bones that lie on the same line. At this point, the cross product of these two normal vectors is equal to zero, meaning that they are parallel along the same line. This is the contact point vector where the resultant contact force is assumed to be acting.

In modeling the behavior of the cartilage, the material characteristics of most significance are the stiffness of the cartilage (in spring-like behavior) and the physical compression of the cartilage in the joint. For two-dimensional models, the plane of observation is the sagittal plane. Along the sagittal plane, the tibio-femoral contact of the knee can be modeled as deformable contact of two bodies. In contact, the meniscus and cartilage are compressed and synovial fluid is squeezed into the knee cavity. Replicating this exact behavior and the non-Newtonian effects of the synovial fluid to the smallest detail, defeats the purpose of a two dimensional model, which should be a simplified version of the actual knee that sufficiently satisfies general knee dynamics and behavior. Adequate results and model integrity for contact can be obtained using the 2D technique of contact overlap (deformable contact formulation). In simple terms, contact overlap is a modeling technique where the meniscus and cartilage are not directly modeled as 2D bodies.

Instead, the cartilage effects are given to the bones. When the bones are pressed against one other, their curve boundaries pass over each other. This overlap of the bone surfaces in the joint represents the area that would have been compressed in the meniscus and cartilage and is called deformable contact formulation.

In 2D models such as the Moeinzadeh model [22], the contact force is calculated by inverse dynamics. In this approach, the ligaments and contact contributions are derived based on external forces. The location of the contact resultant force, in what is called rigid contact formulation, is found by tracing the contact curves of the femur and tibia in search of the location where vectors normal to each curve are aligned. The exact equation used to find the contact vector pair in non-overlapping contact is $n_1 \times n_2 = 0$, where $n_1$is the vector normal to the femur curve, and n_2 is normal to the tibia. The cross product is set to zero because when lines are 180º apart (or parallel), their cross product is zero.

Comparing the two contact formulations, deformable and rigid, a model with contact overlap (deformable) is able to solve for the contact force at each time step in the dynamic motion, utilizing the amount of overlap between the bony structures to determine contact forces.

In the 2D dynamic model developed in this work, the cartilage is modeled using the sagittal deformable contact area approach. The troublesome discovery of multiple contact pairs is found when the vector (or contact points) pair approach is used for the deformable contact modeling. This justified redesigning the contact force method used in the model. The contact curve vectors are shown to have various correct solutions within the same data set. Therefore, it is proposed that it would be more accurate to use the area of deformable overlap and the centroid as a means of obtaining an accurate resultant force. This introduces many challenges in the

dynamic model, but it is necessary to obtain solutions in agreement with a data reported in the literature for certain exercises.

Deformable contact is most accurately modeled if the entire area of contact overlap is fully accounted for, with the centroid of the area used as the basis for locating the resultant contact vector. The overlap area can be found by integrating the difference between the contact curves of the femur and tibia in order to calculate the contact area. This area is similar to a bed of springs sharing the same stiffness. The force is found using $F = k \cdot A$, where A is the area and k is the coefficient of stiffness for the cartilage in N/m^2. This force acts on the tibia and femur equal in magnitude, and opposite in direction, at the centroid of the contact area. The centroid method is consistent at all ranges of contact overlap and varies depending on the distribution of the overlapping area shape.

3.6 Ligaments and Tendons

Ligaments are fibrous structures that connect bones with other bones. The knee has four ligaments connecting the tibia to the femur, ACL, PCL, MCL, and LCL, and the posterior capsule (PC).The ligaments are modeled by a total of 10 fibers, providing stability in the joint and balance. In Ref. [30], the tendons of the knee (connecting muscles to bones) are analyzed for common traits that may lead to patellar tendonitis. Tendons behave much like ligaments do, and consequently are used as the replacement for ligament material in ACL, MCL, and other ligament surgeries. They analyzed the jumping dynamics of professional volleyball players to study what, if any, specific actions led to tendonitis and tendon inflammation. The test setup was a motion capture analysis camera system with force plates and volleyball net. The results of the study showed that rapid, cyclic loading of the tendons in jumping and landing was present in the

tendonitis group. The peak forces were 2 to 3 times body weight when jumping and landing. Thus, in conclusion, for these elite volleyball players, the probability of patellar tendinitis was greatest when high impact forces and rate of force development in the knee extensor mechanism were combined with substantial tibial external torsional moments and deep knee flexion angles.

3.7 Viscoelasticity of Ligaments

Strain rate dependent behavior of the ACL and PCL has been measured and modeled in recent studies [31-34]. Pioletti verified that for a dynamics exercise, the viscoelasticity must be factored into ligament models [32].The nonlinearity, anisotropy, incompressibility, and strain rate related properties of the ligaments are determined. Collagen fibers were characterized by a Kelvin-Voigt viscoelastic behavior [34] with good results. Li [17] used a quasi-linear viscoelastic (QLV) model to predict the stresses and strains in response to loading conditions. The QLV model was able to accurately predict the stress-strain behavior of ligament and tendon. Nekouzadeh [35] also fitted the ligaments, but instead of the QLV model, he used a 1D method to treat the quasi-linearity to reduce computation. The new approach allows relaxation to adapt with the strain history of the ligament, which gave a calibration to this adaptive QLV model. This new approach predicts collagen behavior comparably better than existing models with less computation.

Provenzano [33] argues that nonlinear theory is needed to describe ligaments instead of QLV. He uses rat MCLs to prove that the QLV model has a nonlinear behavior in which the rate of creep is dependent upon stress level and the rate of relaxation is dependent upon strain level. A more general formulation for ligaments is required. In this model an experimental data regression approach is used to implement viscoelastic ligaments. Results from strain rate

material tests [31,33] of cadavers were processed and regression analysis was conducted on the data to compute a factor that could be applied to the ligament forces that accounts for viscoelasticity. The approach reduces computation and is acceptable for a 2D model.

CHAPTER IV

2D ANATOMICAL KNEE JOINT MODEL

4.1 Position Vectors and Coordinate Systems

4.1.1 Position Vectors

The position of all bodies (femur, tibia, and patella) and anatomical points of interest are described using position vectors in this work. Position vectors of insertion points, centers of mass, and points of application of forces that are essential to determine the resultant and moment resultant of each body. A representation of the 2D model is shown in Fig. (2).

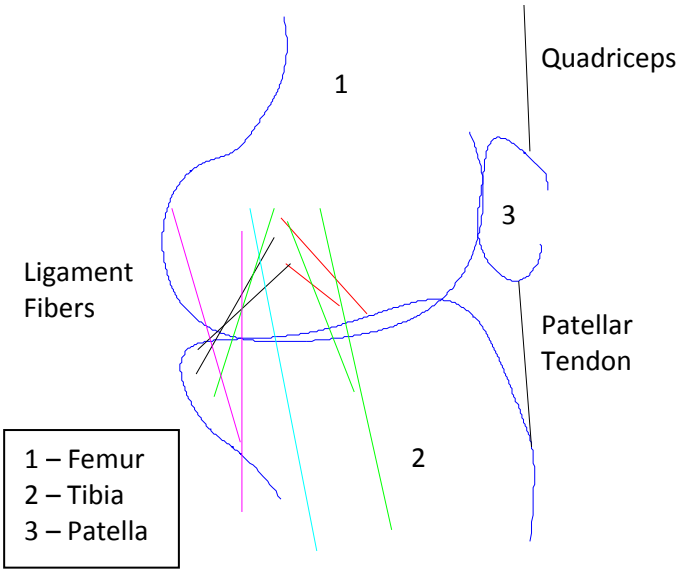

Figure 2: *2D Knee Model as Represented in Matlab*

A force is characterized by magnitude and direction. Analytical relations for ligament forces are developed using position vectors that are parallel to ligament insertion points. Based on the relative position of femur and tibia, the magnitude and direction of the ligament force

along with its moment about the center of mass is determined. The direction of a force is given by a unit vector or normal vector (if contact force) and is shown in Figs. (3) and (4).

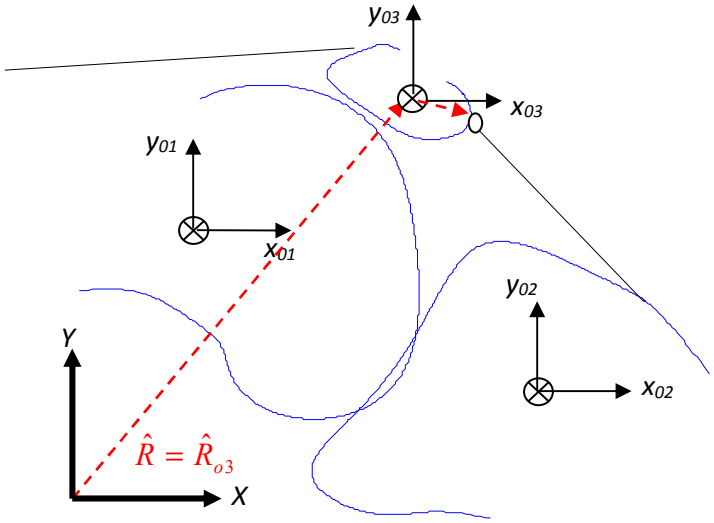

Figure 3: *Bodies with their Embedded Coordinate Systems*

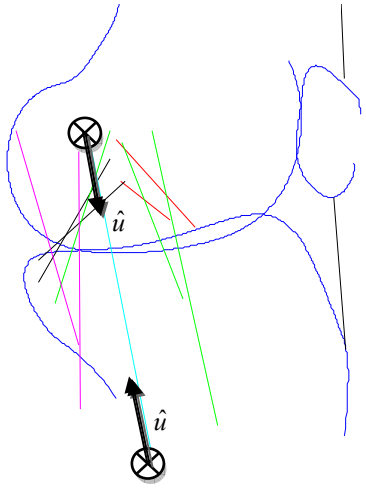

Figure 4: *Unit Vectors Showing Direction of Ligament Force on Femur and Tibia*

To help with the organization and consistency throughout the model, a nomenclature system was created. Because of the number of components involved with the 2D model, it was necessary to distinguish all components. An alpha-numeric variable name was assigned to all position vectors, unit and normal vectors, and forces and moments based on what that variable represents, where it is located, etc.

4.1.2 Coordinate Systems

In describing the coordinate systems used for this 2D Knee Model each body has its own local coordinate system that is embedded into the center of mass of each body and moves with the body as shown in Fig. (3). There are three local coordinate systems - one for each bone. Note that local coordinate systems for femur and tibia in the figure are not actually located at the center of mass, but this is only for illustration purposes. The global coordinate system (fixed in this work) is XY.

4.2 Vector Components Notations

1. *Lower-case letter denotes a **local** vector with respect to a **local** coordinate system.*
2. *Upper-case letter denotes a **global** vector with respect to the **global** coordinate system.*

These rules apply to the first and last letters of the alpha-numeric variable name that describe the position vector (e.g. ***XL1R***, ***yL1r***). An upper case component can be used in conjunction with a lower case position vector. This denotes for instance that a global vectors is represented in a local coordinate system or vice versa (e.g. ***X2Tr*** or ***x2TR***). The system is composed of three bodies and the components that are interconnected with them, as shown in Fig. (2). A number *1*, *2*, or *3* is used to denote with respect to what local coordinate system that position vector belongs to or originates from as shown in Table 1.

4.3 Vector Components of Bony Structures

4. 3.1 Components Notations

Components of vectors are denoted by using a capital or lower-case *X* or *Y* in front of the vector components. The significance of the lower-case or capital letter, as previously mentioned, is to establish whether local or global coordinates are used. (e.g. ***XL1R***, ***xL1r***)

Table 1: *Major Bodies of the model*

Bodies	Representation
1	Femur
2	Tibia
3	Patella
4	Pelvis

Table 2: *Nomenclature identifiers*

Identifier	Denotation
x,X	x-component
y,Y	y-component
N	Normal unit vector
U	Unit vector

4.3.2 Descriptors

Each vector has a distinct descriptor which gives the reader and idea of which object that vector belongs to. (e.g. *XRF4R*, *xL1r*). Descriptors help create families of system variables that can distinguish the variables of one component (ligament) from another (patellar tendon).

Example. *XL2R(n)* – This is a global *X*-component of the ligament insertion point '*L*' with respect to tibia (global coordinate system '*2*') and '*R*' denotes that this is a global position vector. The *(n)* means that there are multiple *XL2R*'s. This is due to the 10 ligaments being modeled.

Example. *xc1r*– This is a local *x*-component of contact '*c*' on femur from tibio-femoral contact and '*r*' denotes that this is a local position vector.

Table 3: *Descriptors*

Descriptor	Denotation
L	Ligament
R	Resultant
F	Force
M	Moment
C	Contact
Q	Quad
W	Wrap
Pt	Patellar Tendon

4.3.3 Position Vectors

A position vector denotes the location of such object with respect to the local coordinate systems of femur, tibia, or patella or the global coordinate system. A position vector is denoted by using, *R* or *r* at the end of the components. A descriptor is added to distinguish the position vectors from other variables in the code.

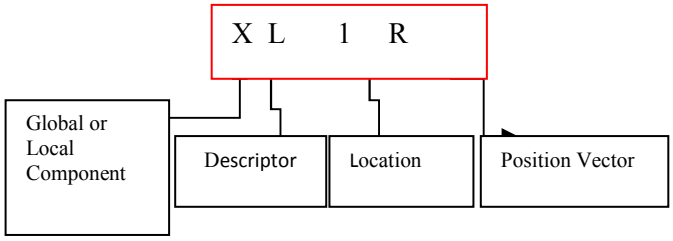

4.3.4 Forces and Moments

A force or moment is denoted by using the identifiers *F* or *M,* respectively, at the beginning of the variable name. A descriptor distinguishes the force or moment, and tells the reader what type of force or moment it is. The number shows where the force or moment is, and from what body the force or moment is originating. Please note that the location is only used when referring to a resultant force or moment. The descriptor is usually enough to distinguish the forces from each other, as certain forces are unique to certain bodies. Finally, the component identifies which axis the force or moment points to. (e.g. *FR1X*, *FC2X*, *MR1Z*)

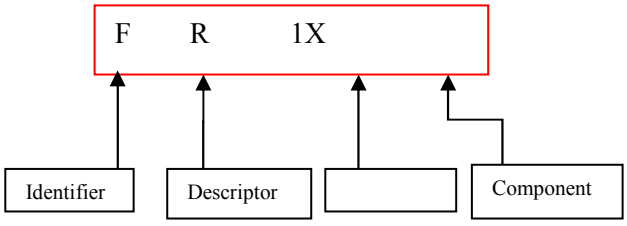

4.3.5 Unit and Normal Vectors

Unit and normal vectors are used to show a direction of interest and to calculate the forces on the knee as well. The notation for these vectors is shown below. The first letter in the series is the identifier; it lets the reader know what they are looking at whether it is a normal vector, etc. The second item in the series is the location; it shows the body the vector is originating from and the body it is pointing to. For example, $\hat{n}_{12}$ is an *x*-component of a normal vector pointing from body 1 to body 2. (e.g. $\hat{n}_{12}$, $\hat{u}_{12}$)

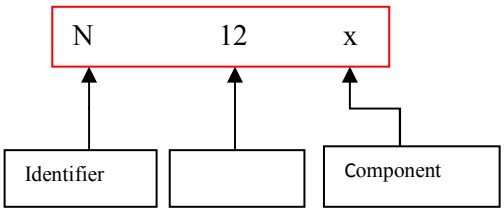

4.3.6 Transformation Matrix

A transformation matrix is used to convert local vectors, a vector that is defined in any of the three local coordinate systems to identify a point of interest, to a global vector. A global coordinate system (a fixed reference frame) is used to keep track of the motion of components of the knee. This global coordinate system is not embedded into the center of masses of the moving bodies, but rather it is found between the femur and tibia in a fixed position as shown in Fig. (3). Since the components of all vectors need to be in the global coordinate system, a transformation matrix is used to transform a vector found in a local coordinate system into a vector with global components. For Eq.(1), *x* and *y* are components of a vector $\hat{r}$ in local coordinate system.

$$\hat{r} = (x, y) \tag{1}$$

In Eq. (2), *X* and *Y* are the components of $\hat{r}$ in the global coordinate system. To transform from local to global coordinates, a rotation matrix is used.

$$\begin{bmatrix} X \\ Y \end{bmatrix} = \overbrace{\begin{bmatrix} \cos\theta & -\sin\theta \\ \sin\theta & \cos\theta \end{bmatrix}}^{T} \begin{bmatrix} x \\ y \end{bmatrix} \tag{2}$$

Here, θ is the angle of the body with respect to the global coordinate system. Hence in the global coordinate system,

$$X = x\cos\theta - y\sin\theta \tag{3a}$$

$$Y = x\sin\theta + y\cos\theta \tag{3b}$$

To transform from global to local coordinates, the inverse of the transformation matrix is used. So from global to local,

$$\begin{bmatrix} x \\ y \end{bmatrix} = \overbrace{\begin{bmatrix} \cos\theta & \sin\theta \\ -\sin\theta & \cos\theta \end{bmatrix}}^{T} \begin{bmatrix} X \\ Y \end{bmatrix} \tag{4}$$

4.3.7 Unit Vectors

Unit vectors are required to calculate the forces in ligaments and tendons. There is a depiction in Fig. (3) that shows $\hat{R}$ as a position vector that denotes the center of mass of a body with respect to a global coordinate system. The following is an example for how to calculate a unit vector for a single ligament; the same procedure is performed to calculate the remainder of the unit vectors used for this model. To locate the position of vector, $\hat{r}_{01}$, on the femur in Fig. (4), the origin of the vector must first be mapped with vector$\hat{R}_{01}$.

$$\hat{R}_{01} = \begin{bmatrix} X_{01} \\ Y_{01} \end{bmatrix} \tag{5}$$

The unit vector, $\hat{u}$, is composed of global components u_x, u_y .

$$\hat{u} = \begin{bmatrix} u_x \\ u_y \end{bmatrix} \tag{6}$$

$\hat{F}$ is the force exerted by body 1 on body 2.

$$\hat{F} = F \cdot \hat{u} \tag{7}$$

$\hat{R}_{i1}$, $\hat{R}_{i2}$are the global position vectors of the insertion points.

$$\hat{u} = \frac{\hat{R}_{i1} - \hat{R}_{i2}}{|\hat{R}_{i1} - \hat{R}_{i2}|} \tag{8}$$

Here, we find the definitions for the terms in Eq. (8).

$$\hat{R}_{i2} = \hat{R}_{02} + \hat{r}_{i2} \tag{9a}$$

$$\hat{R}_{i1} = \hat{R}_{01} + \hat{r}_{i1} \tag{9b}$$

$$\hat{u} = \frac{\hat{R}_{02} + [T_2] r_{i2} - (\hat{R}_{01} + [T_1] r_{i1})}{|\hat{R}_{02} + [T_2] r_{i2} - (\hat{R}_{01} + [T_1] r_{i1})|} \tag{10}$$

where T_1, and T_2 are transformation matrices of body 1 and body 2 respectively. By substituting Eqs. (5 - 9) into (10),

$$\hat{u} = \frac{\begin{bmatrix} X_{02} \\ Y_{02} \end{bmatrix} + \begin{bmatrix} c_2 & -s_2 \\ s_2 & c_2 \end{bmatrix} \begin{bmatrix} x_{i2} \\ y_{i2} \end{bmatrix} - \begin{bmatrix} X_{01} \\ Y_{01} \end{bmatrix} - \begin{bmatrix} c_1 & -s_1 \\ s_1 & c_1 \end{bmatrix} \begin{bmatrix} x_{i1} \\ y_{i1} \end{bmatrix}}{\left| \begin{bmatrix} X_{02} \\ Y_{02} \end{bmatrix} + \begin{bmatrix} c_2 & -s_2 \\ s_2 & c_2 \end{bmatrix} \begin{bmatrix} x_{i2} \\ y_{i2} \end{bmatrix} - \begin{bmatrix} X_{01} \\ Y_{01} \end{bmatrix} - \begin{bmatrix} c_1 & -s_1 \\ s_1 & c_1 \end{bmatrix} \begin{bmatrix} x_{i1} \\ y_{i1} \end{bmatrix} \right|} \tag{11}$$

where s_2, c_2 , are the sine and cosine of θ_2.The unit vector *x* and *y*-components are given by:

$$A = X_{02} + c_2 x_{i2} - s_2 y_{i2} - X_{01} - c_1 x_{i1} + s_1 y_{i1} \tag{12a}$$

$$B = Y_{02} + s_2 x_{i2} + c_2 y_{i2} - Y_{01} - s_1 x_{i1} - c_1 y_{i1} \tag{12b}$$

$$u_x = \left[\frac{A}{\sqrt{A^2 + B^2}} \right] \tag{13}$$

$$u_y = \left[\frac{B}{\sqrt{A^2 + B^2}} \right] \tag{14}$$

4.3.8 Moment of a Force

The moment arm of a force is considered with respect to the center of mass of a body. $\overline{X}$ and $\overline{Y}$ are components w.r.t the global system as shown in Fig. (5). $\hat{R}$ is the global position vector with respect to the center of mass of the body and $\hat{r}$ is the local position vector

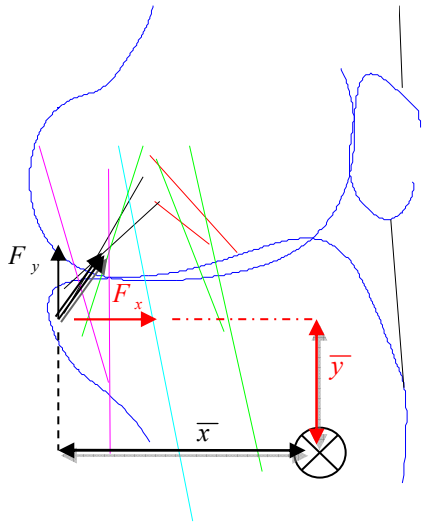

Figure 5: *Calculation of a Moment of a Force on Tibia*

$$\hat{r} = \begin{bmatrix} x_i \\ y_i \end{bmatrix} \tag{15}$$

where, x_{i1} , y_{i1} are the local coordinates of the insertion point of the ligament or tendon on femur. Ligaments and tendons exert a pulling force $\hat{F}$ given by,

$$\hat{F} = F \cdot \hat{u} \tag{16}$$

Where $\hat{u}$ is the unit vector given by Eqs. (13, 14) and u_x, u_y are the global components of the unit vector of a force from one body to the other body as shown in Fig. (3). The moment of a force with respect to the center of mass of the body is given by the formula:

$$M_c(\hat{F}) = \{[T]\hat{r}\} \times \hat{F} \tag{17}$$

Transforming $\hat{r}$ to the global coordinate system, and substituting Eq. (16) into (17):

$$M_c(\hat{F}) = [T] \cdot \hat{r} \times F \cdot \hat{u} \tag{18}$$

$$M_c(\hat{F}) = F \cdot \begin{bmatrix} c & -s \\ s & c \end{bmatrix} \hat{r} \times \hat{u} \tag{19}$$

Where *c* and *s* are the cosine and sine of θ, which is the angle of the body with respect to the global coordinate system; the moment can be calculated by substituting Eqs. (6) and (15) into (19). The resulting equation is as follows:

$$M_c(\hat{F}) = F\begin{bmatrix} c & -s \\ s & c \end{bmatrix}\begin{bmatrix} x_i \\ y_i \end{bmatrix} \times \begin{bmatrix} u_x \\ u_y \end{bmatrix} \tag{20}$$

$$M_c(\hat{F}) = F\begin{bmatrix} cx_i - sy_i \\ sx_i + cy_i \end{bmatrix} \times \begin{bmatrix} u_x \\ u_y \end{bmatrix} \tag{21}$$

$$M_c(\hat{F}) = F\begin{vmatrix} \hat{i} & \hat{j} & \hat{k} \\ cx_i - sy_i & sx_i + cy_i & 0 \\ u_x & u_y & 0 \end{vmatrix} \tag{22}$$

$$M_c(\hat{F}) = F\left[(cx_i - sy_i)u_y - (sx_i + cy_i)u_x\right]\hat{k} \tag{23}$$

4.4 Anatomical curves

The anatomical curves are parametric equations that represent the bones or bodies in the knee: femur, tibia, and patella in Matlab. These curves have been developed using digitalization of *x*-rays of the knee joint in the sagittal plane.

4.4.1 Femoral Curve

In Eq. (25), the coordinate X_f is the *x*-coordinate of the femoral curve and *XCOFE* are the *x*-coefficients of femoral curve. Previous studies were referenced to determine the values for the x-coefficients.

$$X_f = XCOFE \cdot a_F \tag{24}$$

$$X_F = XCOFE \cdot \overbrace{\begin{bmatrix} u^0 & u^1 & u^2 & u^3 & u^4 & u^5 & u^6 & u^7 & u^8 & u^9 & u^{10} \end{bmatrix}^T}^{a_F} \tag{25}$$

Thus the *x*-coordinate equation reduces to Eq. (26) and is a function ofu_F, the *u*-parameter of the femoral curve from 0 to 1 which progresses along the curve from beginning to end as shown in Fig. (6).In other words, the *u*-parameter is a linearly spaced vector from zero to one used to find the curvature of the bones.

$$x(u_f) = a_0u^0 + a_1u^1 + a_2u^2 + \cdots + a_9u^9 + a_{10}u^{10} \tag{26}$$

Similarly we obtain equation, Y_f, which is the *y*-coordinate of femoral curve,

$$Y_f = YCOFE \cdot b_F = y(u_f) = b_0u^0 + b_1u^1 + b_2u^2 + \cdots + b_9u^9 + b_{10}u^{10} \tag{27}$$

By plotting the coordinates of y_f vs. x_f, the femoral curve is obtained as shown in Fig. (6). The femoral curve arrays in this orientation of the bone will generate clockwise data.

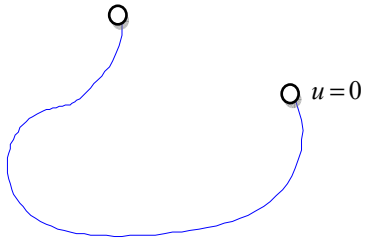

***Figure 6**: The Femoral Curve*

4.4.2 Tibial Curve

The tibia's bone curve is generated very similarly to the femur, with the exception of differently notated terms in the equations. X_t is the *x*-coordinate of tibial curve, while $XCOTI$ and $YCOTI$ are the *x* and *y* coefficients, respectively. Following the procedure used for the femur, the tibia curves are described in Eqs. (28) and (29).

$$X_t = XCOTI \cdot a_t = y(u_t) = a_0u^0 + a_1u^1 + a_2u^2 + \cdots + a_9u^9 + a_{10}u^{10} \tag{28}$$

$$Y_t = YCOTI \cdot b_t = y(u_t) = b_0u^0 + b_1u^1 + b_2u^2 + \cdots + b_9u^9 + b_{10}u^{10} \tag{29}$$

Plotting Y_t vs.X_t the tibial curve is obtained as shown in Fig. (7).

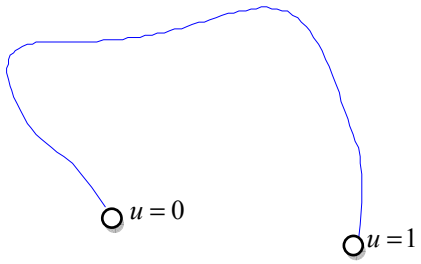

Figure 7: *The Tibial Curve*

The tibial and femoral curves generated are for standing position. For different positions, rotation matrices are applied on the arrays of (*X*, *Y*) anatomical curve coordinates, and addition and subtraction (for *X*,*Y* translation), are used to properly position the tibial and femoral curves.

4.4.3 Patellar Curve

The patellar anatomical curve is found in a similar manner to tibia and femur. The following equations illustrate the patellar curve. x_P is the *x*-coordinate of patella and is a constant. $y_P$varies with the u_P from zero to one with Eqs. (30a) and (30b).

$$X_p = XCOPA \cdot a_p = y(u_p) = a_0u^0 + a_1u^1 + a_2u^2 + \cdots + a_9u^9 + a_{10}u^{10} \quad (30a)$$

$$Y_p = YCOPA \cdot b_p = y(u_p) = b_0u^0 + b_1u^1 + b_2u^2 + \cdots + b_9u^9 + b_{10}u^{10} \quad (30b)$$

By then plotting $y_P$vs.x_P, the femoral curve is obtained as shown in Fig. (8).

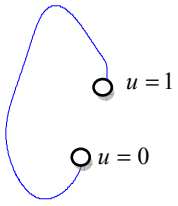

Figure 8: *The Patellar Curve*

4.4.4 Initial Position of Curves

Once the curve data for the bones is in the model, the final step is to rotate and translate the curves to their initial positions for testing. The final position for a standing test is shown in

Fig. (9). The position is not the exact one used in testing, but shows that any 2D position can be selected at any rotation angle for these bones.

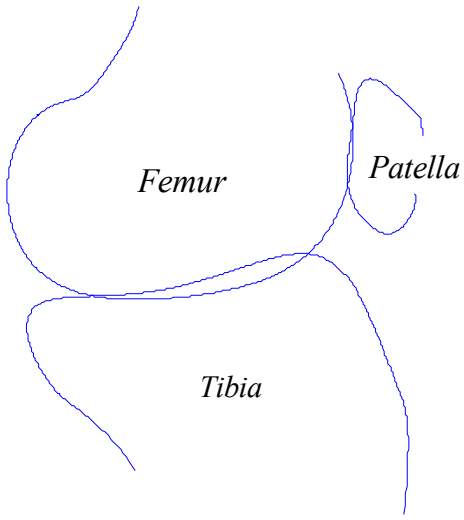

Figure 9: *Bones of Knee Model, Plotted in Standing Position*

4.5 Model Structure for Simulations

The knee model is separated into individual functions to help in debugging and to make it flexible for the simulations to be conducted using Matlab. For dynamic testing, the solver *ode15s*function is called in *Main*. *Main* is where the initial conditions for the test are defined, such as input variables for masses and lengths of the bones. The solver in *Main* requires a second function, which contains the differential equations of the system that are to be solved. In this model, the differential equations include algebraic constraints that form a set of differential algebraic equations (DAE).This DAE system is described in the *DAE System* function, which calls *Bones* for calculations of forces and moments in the system.

In Fig.(10), the model code structure is shown as is built in Matlab. The structure of the code is tiered from left to right, with the functions on the left calling the functions directly to their right for specific operations. The functions were all developed, with the exception of

Intersections, which is from the Matlab file exchange. This design allows the model researcher to make changes to a specific function within the code without affecting the surrounding functions. In the following chapters the functions are detailed to explain the procedures within *Contact*, *Ligaments*, *Tibia*, *Femur* and the *DAE System*. Because this is a dynamic model, the main variables that are being tested are 1) the coordinates of the center of mass X and Y and orientation angle θ with respect to the global coordinate system for each body, and 2) their derivatives. The derivatives are the velocities and accelerations of the dynamic system of equations.

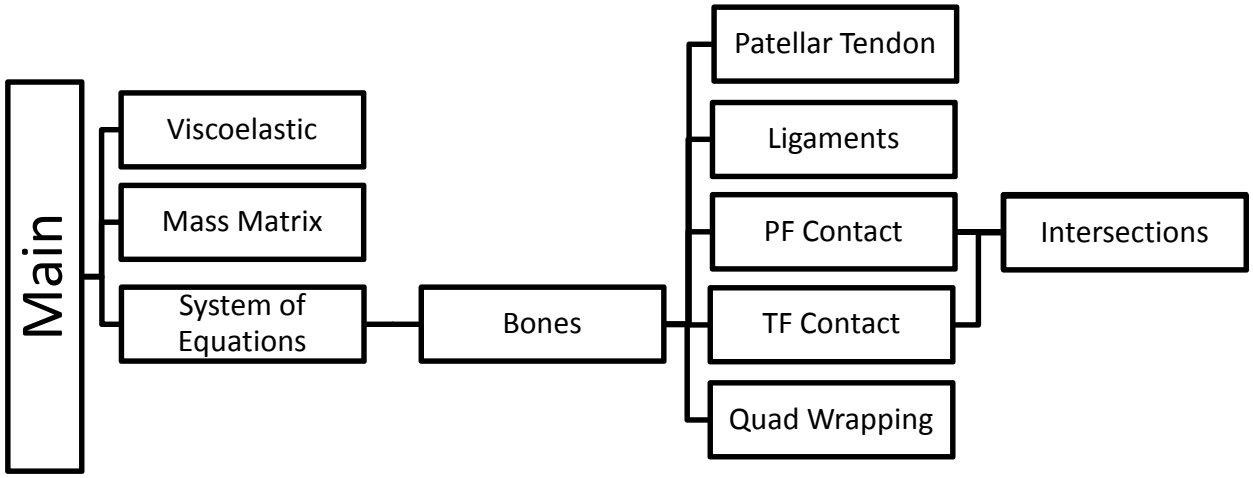

Figure 10: *Structure of the Dynamic Model*

4.5.1 Main

Main is the function that contains all the primary input variables of the model, such as the testing frequency, bone material properties (mass, moment of inertia, etc.), cartilage stiffness coefficients, initial (x_0) bones positions, orientations and corresponding velocities, testing time (sec), forces applied to the knee, viscoelastic constants, deficiencies of ligaments, and bone constraints, in addition to many other input options. This function will run the model and will call the *Mass Matrix* function and establish the differential algebraic equation system for solver *ode15s* in Matlab.

4.5.2 Mass Matrix

Main calls the mass matrix one time. This matrix will vary depending on the number of ligaments being tested, as this changes the number of system variables. *Mass Matrix* is built as a large mass matrix of currently up to 42 x 42 entries in the model. The matrix is essential for the system of differential algebraic equations to be solved, and is different for each exercise being performed. Depending on the experiment identified in *Main*, the mass matrix has been programmed to adapt to what is requested and provide itself to the *DAE System*.

4.5.3 DAE System

This function contains the primary equations that define an experiment of the knee model. There are 42 equations in total, which can be downsized to 28 or 12 equations depending on testing conditions such as the elastic mode of ligaments, deficient ligaments, and viscoelastic ligaments. The system of equations solves each equation for either a velocity or acceleration for the first 12 terms, and either a strain or strain rate of a ligament for the last 20 terms if the model is being tested with viscoelastic ligaments and no patella, described in Chapter 5.

4.5.4 Viscoelastic

Viscoelastic ligaments solves for all the model conditions of viscoelasticity for *Ligaments*. This code is called by *Main* just one time if viscoelasticity is called for at the beginning and the resulting variables are stored as global variables. These variables in *Viscoelastic* ligaments include the insertion points of the ligaments, the ligament stiffness', slack lengths, and anatomical data of the knee ligaments. An entire strain rate dependent interpolation based on experiments on human cadaver knees (from the literature) is performed in *Viscoelastic* to apply the effects of strain rate on the tensile forces of the knee when the ligaments are

activated. The result are coefficients that are used at each knee position and strain rate of motion to calculate the forces in the ligaments as a function of the strain rate each one is experiencing.

4.5.5 Bones

Bones is called by the *DAE system* to find all the forces needed in the 42 system equations that are being solved for at each step in the code's iteration. The function *Bones* will call on two sub functions *Contact* and *Ligaments* to provide the contact force and ligament forces at the current knee position. One can think of this position as a snapshot in time that is being solved for all the forces and moments in a complex motion. *Bones* takes all the resulting force vectors acting on the tibia and femur, and solves for the summation of forces along the center of mass of each bone. These equations turn the local position vectors into global vectors and provide the values necessary in *DAE System*.

4.5.6 Ligaments

Bones will call on *Ligaments* to solve for the forces and moments generated by the ligaments in the model. In *Ligaments*, the insertion points of the ligaments in the bones are calculated and used to find the amount of stretch in the ligaments. Above a certain strain threshold, the ligaments become load bearing, and as viscoelastic materials, their load bearing abilities change with the rate of loading. Therefore, *Bones* will call on the global variables from *Viscoelasticity*, and solve these equations using the current position in the model, therefore solving for the effect of the strain rate on the ligaments and the resulting force. The ligament force calculations vary in *Ligaments* depending on the conditions being tested, and global variables from *Main* will dictate what conditions are being tested.

4.5.7 Patello-Femoral and Tibio-Femoral Contact

PF-Contact and *TF-Contact* are the largest functions in the code and the most complex. The contact functions take the crude bone profile curves and uses *Intersections* to find if the bones intersect. Once the bones intersect, a highly defined bone mesh is applied to significantly improve the accuracy of the model while reducing the computation time. This allows for the creation of local arrays of the contacting curves of the tibia and femur that are between the intersection points and have 100 points that are linearly spaced and highly defined. These local contact curves are then rotated and curve fitting is used to develop equations that represent the curves. These equations, or functions, are then integrated using *trapz* to find the areas below the curve in the local rotated coordinate system. The data in this system is standardized for numerical computation, which helps to solve for the curves. Afterwards, the new curves are unstandardized and rotated back to global scale and the centroid of the areas are found and used to generate the contact force at that knee position. After the force vector is applied, the unit vector location is found using the centroid for the moment calculations. This calculation is performed in *TF-Contact* and *PF-Contact* and supplied to *Bones*.

4.5.8 Intersections

Intersections is a code from the Matlab Exchange that will take an array of points that form two separate lines and can tell you if and where exactly these two lines intersect. This is critical for *Contact*. Function *Intersections* is called upon to locate the intersection points that may exist as the bones come into close positions during the exercises. This code has been thoroughly tested during this research, and is extremely robust and accurate. It is not all knowing, and sometimes there are many intersection points occurring, and or strange positions of the knee with an odd number of intersection points, but these situations are have been tested and

the code has been written so that these conditions are dealt with accordingly, accurately, and will not trip the model solver (*ode15s*).

4.5.9 Patellar Tendon

The patellar tendon is a function that locates the patellar tendon insertions on the patella apex and tibial tuberosity. It treats the patellar tendon similar to a ligament and viscoelasticity is applied. Since data is limited and the tendon resembles a very stiff ligament, the assumption was made to use the PCL anterior fiber viscoelastic response on the patellar tendon for system dampening. The PCL anterior has the most stiff viscoelastic response of the ligaments, so this was an assumption for the patellar tendon viscoelasticity.

4.5.10 Quadriceps Wrapping

For large flexion angles the femoral condyle comes into contact with the quadriceps tendon and causes the tendon to wrap around. The wrapping points along the femur depend on patellar flexion. Perpendicularity of unit vectors, perpendicular to femoral condyle surface and along patellar tendon, is the approach used to find the wrapping point.

4.6 Modeling of Ligaments

4.6.1 Modeling Ligaments

The ligaments (and their fibers) play an important role in limiting the range of motion between femur and tibia. Their purpose in the knee is to control the passive multi-directional stability. In the 2D model, the inner knee ligaments are modeled as nonlinear spring elements that are pin connected on each bone. This replicates the actual behavior of a ligament with the assumption that the ligament connects to the bone at a point, instead of a three-dimensional surface area. The insertion points of the ligament fibers are critical to model performance and

were found experimentally in a cadaver measurement study [36]. The insertions for the ligaments were obtained using Roentgen Stereophotogrammetry.

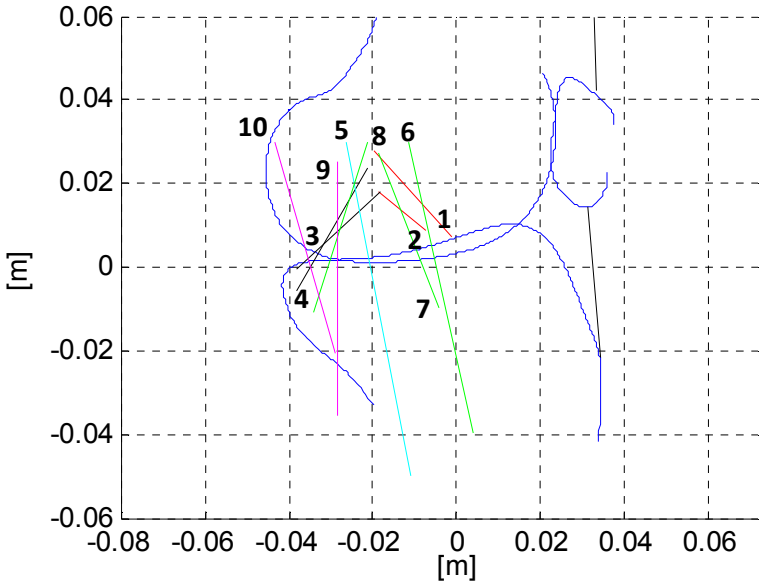

Figure 11: *Ligaments Fibers in 2D Model*

Table 4: *Ligament fibers*

1	ACLant	6	MCLant
2	ACLpos	7	MCLdeep
3	PCLant	8	MCLoblq
4	PCLpos	9	PSCAPmed
5	LCL	10	PSCAPlat

Table 5: *Ligament insertion points*

Ligament	XL1R	YL1R	XL2R	YL2R
ACLant	-0.020	0.028	-0.001	0.007
ACLpos	-0.019	0.018	-0.007	0.009
PCLant	-0.018	0.018	-0.038	-0.000
PCLpos	-0.021	0.024	-0.038	-0.006
LCL	-0.027	0.030	-0.011	-0.050
MCLant	-0.012	0.030	0.004	-0.040
MCLdeep	-0.019	0.027	-0.004	-0.010
MCLoblq	-0.022	0.030	-0.034	-0.011
PSCAPmed	-0.029	0.025	-0.028	-0.036
PSCAPlat	-0.044	0.030	-0.029	-0.021

As discussed earlier, the main ligaments of the knee are the ACL, PCL, MCL, and LCL. These ligaments and posterior capsule are modeled as the 10 fibers, which are listed in Table 4. Insertion points for these ligaments relative to tibia and femur center of mass are given in Table 5 in the unit of meters. Each of the ligaments has a known unstretched length and slack length that are used for finding if the ligament is loaded or unloaded at a position of the knee, Fig. (12).

In this work the ligament testing exercise is simulated using the straightforward 2D model for a proximal-distal motion of the tibia under soft excitation. Movements in the anterior and posterior directions are primarily stabilized by the ACL and PCL. Therefore, the ACL and PCL are expected to carry the highest loads in anterior-posterior displacement tests.

To obtain the ligament forces of the dynamic knee model shown in Fig. (13), a global coordinate system as shown in green in Fig. (12) is established. The local position vectors of the insertion points of a ligament on the femur and tibia are $\bar{r}_A$and$\bar{r}_B$, Fig. (12). To obtain the global components of local vectors $\bar{r}_A$ and $\bar{r}_B$, the two vectors must be multiplied by their transformation matrices shown in Eq. (31).

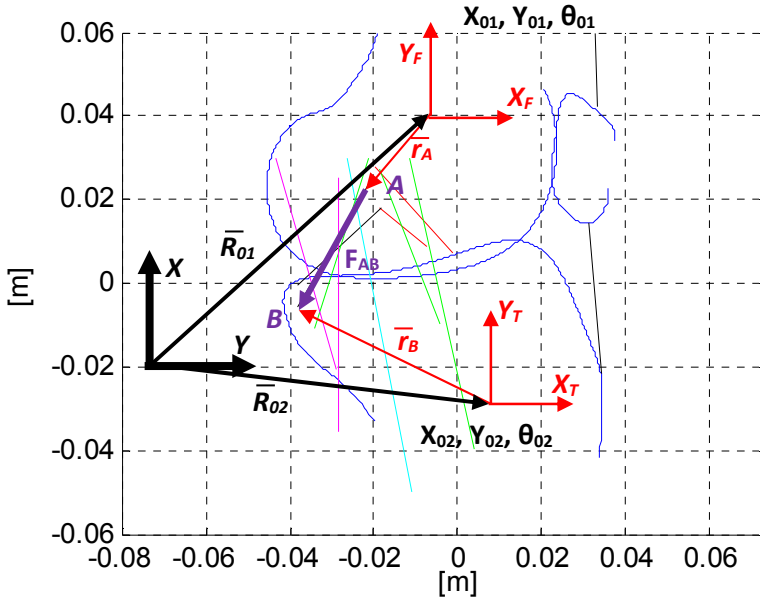

Figure 12: *Knee Vectors in Ligament Modeling*

$$[T_n] = \begin{bmatrix} \cos\theta_n & -\sin\theta_n \\ \sin\theta_n & \cos\theta_n \end{bmatrix} \tag{31}$$

The n in Eq. (31) is the number of the body rotated by θ_n. For instance, for the ligament forces that act between the femur and the tibia, bodies 1 and 2, respectively, the local coordinates must be transformed such that the transformation matrix will rely on angle θ_1 for the femur and θ_2 for the tibia.

The global vectors in Fig. (12) for the centers of mass of the femur and tibia are $\bar{R}_{01}$ and $\bar{R}_{02}$, respectively. Capitalizing R indicates a global vector, and subscripting 01 indicates the origin of the local coordinate system of body 1. To find the representation of Fig. (12) for vector $\overline{AB}$ in global coordinates, the following equation results:

$$\overline{AB} = \bar{R}_{02} + [T_2]\bar{r}_B - \bar{R}_{01} - [T_1]\bar{r}_A \tag{32}$$

Expanding Eq. (32) into its x and y vector components and transforming vectors $\bar{r}_A$and $\bar{r}_B$, $\overline{AB}$ can be rewritten as Eq. (33).

$$\overline{AB} = \begin{bmatrix} \mathrm{X_{AB}} \\ \mathrm{Y_{AB}} \end{bmatrix} = \begin{bmatrix} \mathrm{X_{02}} + \mathrm{x_B}\cos\theta_2 - \mathrm{y_B}\sin\theta_2 - \mathrm{X_{01}} - \mathrm{x_A}\cos\theta_1 + \mathrm{y_A}\sin\theta_1 \\ \mathrm{Y_{02}} + \mathrm{x_B}\sin\theta_2 + \mathrm{y_B}\cos\theta_2 - \mathrm{Y_{01}} - \mathrm{x_A}\sin\theta_1 - \mathrm{y_A}\cos\theta_1 \end{bmatrix} \tag{33}$$

From Eq. (33), the vector $\overline{AB}$ is separated into X and Y-components and the ligament insertions into the bones are located in global coordinates.

4.6.2 Ligament Forces

Certain ligament fibers restrain the relative motion between femur and tibia, while others may remain untensioned. As seen in Fig. (12), the force F_{AB}represents the force in the ligament acting on the vector $\overline{AB}$ from point A on the femur, to point B on the tibia. The ligament force, $\bar{F}_{lig}$, is:

$$\bar{F}_{lig} = F_{lig} \cdot \bar{U} = F_{lig}(U_X\bar{\imath} + U_Y\bar{\jmath}) \tag{34}$$

The magnitude of the inelastic ligament force varies in accordance to the strain ε of the ligament. In this model, the ligaments are treated as nonlinear springs. The nonlinear behavior for these ligament springs is one such that initially the ligament strains easily until hitting a threshold, after which there is increased resistance to elongation. This nonlinear stress-strain relationship is subdivided into three regions for modeling. Depending on the amount of strain on the ligament relative to its linear range threshold, ε_0 [4], the force can be found as a function of strain conditions. Ligaments follow the three cases that are provided below:

Case 1. If the ligament is not being strained, force will be zero.$\varepsilon \leq 0$.

$$\bar{F}_{lig} = 0 \tag{35}$$

Case 2. If the strain falls between $0 < \varepsilon < 2\varepsilon_0$, there is quadratic behavior.

$$F_{lig} = k_q \left(\sqrt{X_{AB}^2 + Y_{AB}^2} - L_0\right)^2 \tag{36}$$

Case 3. If $2\varepsilon_0 \leq \varepsilon$, the slope is assumed to be linear (linear region):

$$F_{lig} = k_L \left(\sqrt{X_{AB}^2 + Y_{AB}^2} - (1 + \varepsilon_0)L_0\right) \tag{37}$$

4.6.3 Moment of Ligament Force

The force acting in a ligament fiber generates a moment with respect to the center of mass. The moment of a force is given by $\bar{M} = \bar{r} \times \bar{F}$. The equation for the moment of the ligament force, Fig. (12), on the femur is as follows:

$$M(\bar{F}_{lig}) = [T_1]\bar{r}_A \times F_{lig}\bar{U} \tag{38}$$

Substituting the transformation matrix from Eq. (31) into Eq. (38), the moment becomes:

$$M(\bar{F}_{lig}) = F_{lig}\bar{U}_y(x_A \cos\theta_1 - y_A \sin\theta_1) - F_{lig}\bar{U}_x(x_A \sin\theta_1 + y_A \cos\theta_1) \tag{39}$$

The moments of the ligament forces are summed about the center of mass of the body, and the overall moment contribution from the ligament forces on the bone is found.

4.6.4 Ligament Force Testing

Once the ligament force equations were included into the knee model, along with ligament insertion points, stiffness coefficients, and slack lengths, the ligaments were tested for accuracy. The knee model forces were first calculated by hand using the governing system equations and then compared to the numerical results. Various knee rotations were tested to make sure every aspect of the code was robust. Numerical simulations matched analytical calculations. The following results for one of the knee position tests (anterior/posterior displacement exercise) are reported.

Fig. (13) shows that during the ligament testing from an initial standing position, if the tibia is displaced from 0-2cm posteriorly, the X-component forces in the PCL ligaments increase greatly, while other ligaments are seemingly unaffected. As expected, it is the ACL and PCL that experience restraining forces when shifted posteriorly with the PCL force increasing the entire way, and ACL being strained only after a centimeter of displacement, suggesting that the ACL begins in an unstrained position before eventually reaching a tensed state in the X direction.

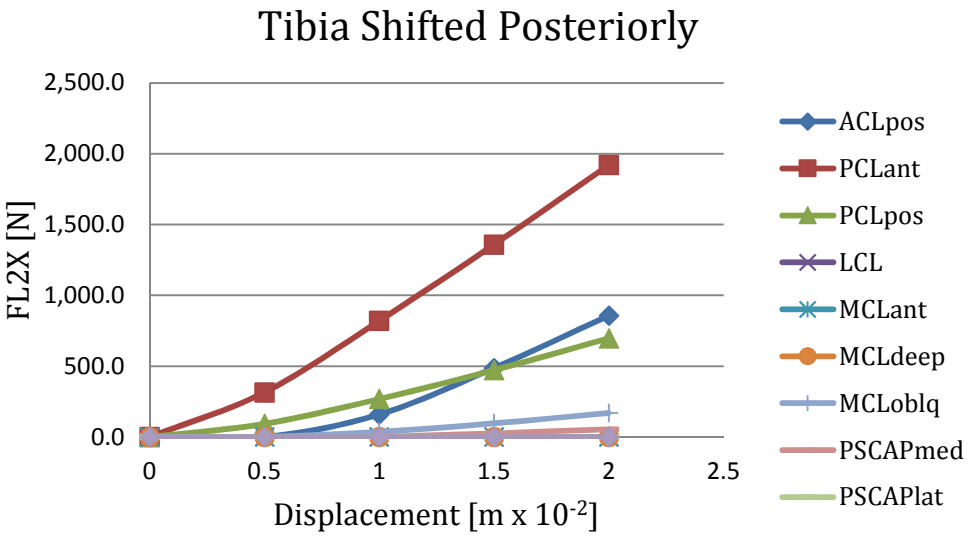

Figure 13: *Posterior Displacement of Tibia (X-component)*

When strained posteriorly, Fig. (14), the Y-components of the ligament forces react as would be expected, with the ACL and PCL having the greatest Y-component forces. The PCL sees the increase in the Y-component first, while the LCL and MCL see hardly any response from this tibial translation.

Fig. (15) shows that the moment sum of the forces in the ligaments with respect to tibia when posterior/anterior displacement occurs is initially negative and then after reaching a no tension normal position, the moment changes its sign. This fits experimental ligament behavior from studies such as [37] and further validates the ligaments in our model. Additionally, the forces shown in Figs. (13-15) are all in the same range of experimental ligament tensile tests done on human cadaver knees. The ligament force results are very accurate when compared against experimental results at the same testing conditions [38]. Additional tests were done for anterior motion with positive results.

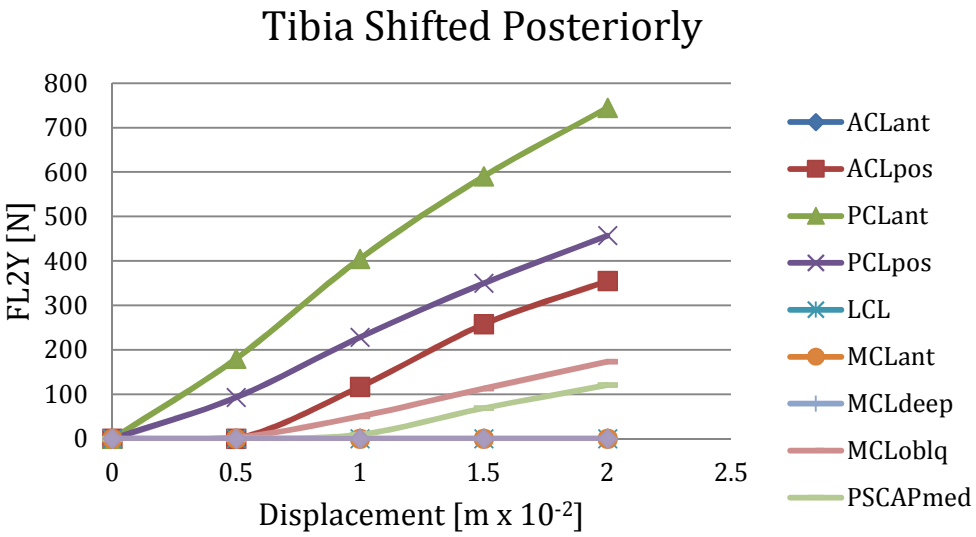

Figure 14: *Posterior Displacement of Tibia (Y-component)*

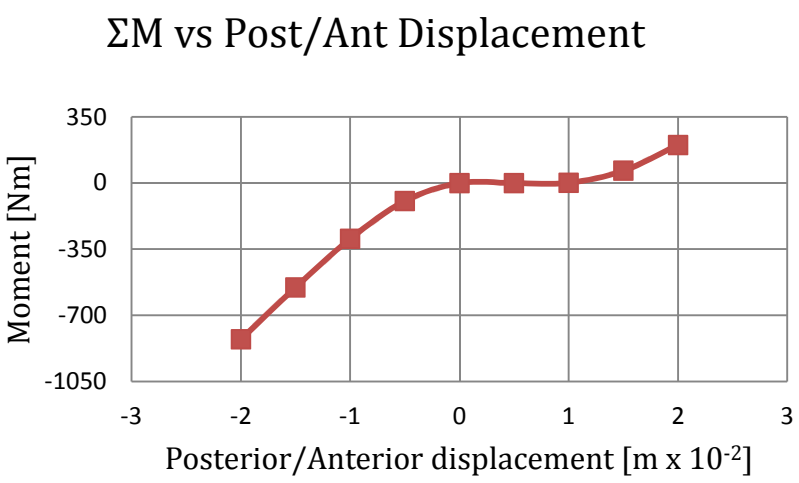

***Figure 15**: Sum of Moments on Tibia for Anterior/Posterior Displacements*

4.7 Viscoelastic Ligaments

After testing of the knee model using elastic ligaments in high ligament strain rate exercises, it became clear that it was critical for the ligament model to include viscoelastic effects. The ligaments have different mechanical properties depending on the strain rate [31-33]. Failing to include viscoelastic effects generates an unrealistic elastic model. To account for viscoelasticity, the model of this work was appended to include an extensive literature review of strain rate effects on ligaments [27, 31-34, 54]. These effects were quantified at different strain rates, and viscoelastic effects on ligaments were applied to our model using regression.

4.7.1 Modeling Viscoelasticity

The main idea for the viscoelastic ligaments is to make our current, one-dimensional elastic ligaments take strain rate into account without over-complicating the model. The stress-strain relationships of ligaments vary at different strain rates. This relationship can be seen in Fig. (16). The curves follow a visible pattern with the toe region initially quadratic, and then as strain increases, the stress-strain response becomes linear. This resembles one side of a parabola and as the strain rate increases, the steepness of the curve increases.

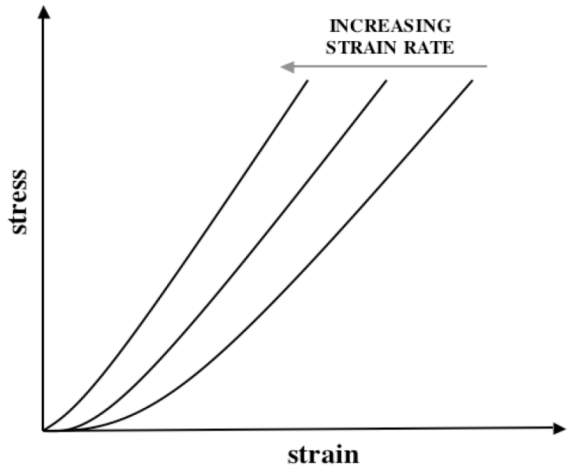

Figure 16: *Strain Rate Effect on Stress* [34]

In Fig. (17), one can see the idea of introducing the viscoelastic behavior in the ligament model. A parabola can be transformed into a family of parabolas by multiplying it by a coefficient. One can make the parabola steeper or wider depending on the value of the coefficient. Using the concept illustrated in Fig. (17), a procedure for finding the strain rate effect on the ligament is developed. To do this, the ligaments' elastic force is multiplied by a factor dependent on the strain rate of each ligament. This factor is found using polynomial interpolation of experimental data. This is explained in 4.7.2 Regression Methodology.

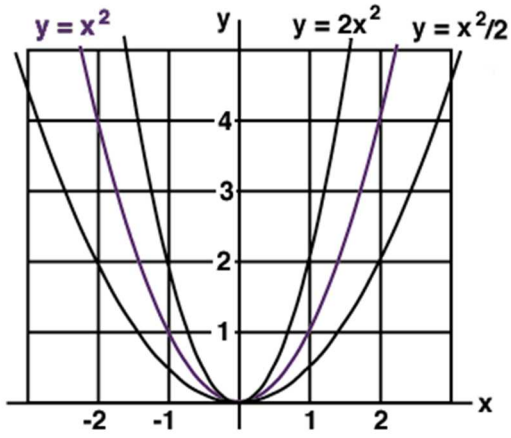

Figure 17: *Effect of Leading Coefficient on a Parabola,* $y = ax^2$

4.7.2 Regression Methodology

The mathematical approach used to calculate the curve multiplication factor is regression analysis. First, an extensive literature review was performed to find the material characteristics of the ACL [2], PCL [2], MCL [11], and LCL [31-34]. Both whole ligaments and separated ligament fibers were included in the search. Once these stress-strain plots were gathered the figures had to be converted into Matlab arrays. This was achieved using a Matlab File Exchange program called *Grab-It*. Grab it takes a figure and allows the user to pinpoint the axis origins and values and then proceeds to transcribe any chosen points into a Matlab array of *x* and *y* coordinate pairs. Once all the plots were transcribed for the ligaments, the ACL was chosen to be the initial testing ligament for the analysis, which would then serve as the model for the rest of the fibers.

The strain rate is the independent variable of the coefficient that will dictate the amount of curvature adjustment required. The equation we use is: $F_{ViscoElastic} = \alpha \cdot F_{Elastic}$, where α is the coefficient and it found using a separate equation. To findα, regression analysis is conducted. Minimizing the error between experimental curve and the best-fit curve at different strain rates leads to α. For each strain rate of a ligament a coefficient α_n is determined. This is shown in Eq. (40), where f_1 results from is model best fit for the experimental data, $\hat{f}_2$, from literature.

$$\alpha_n = \frac{\sum_{i=1}^{\#pts} \hat{f}_2 f_1}{\sum_{i=1}^{\#pts} {f_1}^2} \tag{40}$$

Figure (18) shows what exactly $\hat{f}_2$ and f_1 represent for general curves. In the figure below, the α will be larger than one, and increase with higher strain rates.

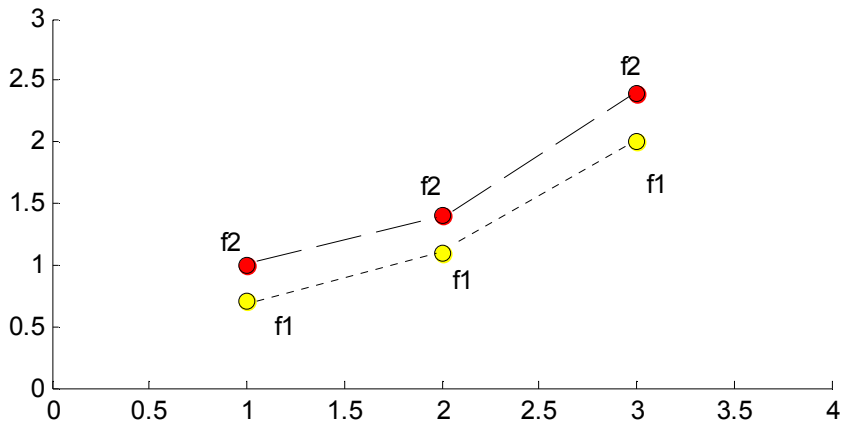

Figure 18: *Strain Rate Dependent Curves (f_2>f_1)*

Once α_n values are found for a ligament at various strain rates we must be able to draw a conclusion from the pattern to find the strain rate effect on the ligament. For example, there was another curvef_3 at a higher strain rate than f_2, and then a curve f_4 at an even higher strain rate, then there will be a set of α's that regression coefficients. The model is then assumed as $F_{ViscoElastic} = [\boldsymbol{C_0 + C_1\dot{\varepsilon}_1 + C_2(\dot{\varepsilon}_1)^2 + C_3(\dot{\varepsilon}_1)^3}] \cdot F_{Elastic}$, where these C coefficients of the interpolation polynomial have to be determined by solving a linear system of equations as follows

$$\boldsymbol{C_0, C_1, C_2, C_3} \xleftarrow[\boldsymbol{SolvingLinearSystem}]{} \begin{cases} \boldsymbol{\alpha_1 = C_0 + C_1\dot{\varepsilon}_1 + C_2(\dot{\varepsilon}_1)^2 + C_3(\dot{\varepsilon}_1)^3} \\ \boldsymbol{\alpha_2 = C_0 + C_1\dot{\varepsilon}_2 + C_2(\dot{\varepsilon}_2)^2 + C_3(\dot{\varepsilon}_2)^3} \\ \boldsymbol{\alpha_3 = C_0 + C_1\dot{\varepsilon}_3 + C_2(\dot{\varepsilon}_3)^2 + C_3(\dot{\varepsilon}_3)^3} \\ \boldsymbol{\alpha_4 = C_0 + C_1\dot{\varepsilon}_4 + C_2(\dot{\varepsilon}_4)^2 + C_3(\dot{\varepsilon}_4)^3} \end{cases} \quad (41)$$

From this point, it can be easily acquired the viscoelastic forces in the ligaments by just plugging in a strain rate into $F_{ViscoElastic} = [\boldsymbol{C_0 + C_1\dot{\varepsilon}_1 + C_2(\dot{\varepsilon}_1)^2 + C_3(\dot{\varepsilon}_1)^3}] \cdot F_{Elastic}$.

4.7.3 Splitting Ligaments into Fibers

Most of the data in the literature on viscous ligaments reports the ligament behavior as a whole, rather than as its fibers. For example, Pioletti [32] tests the whole ACL ligament and

whole PCL ligament at various strain rates. In order to use Pioletti's results in the presented viscoelastic model which includes 10 ligament fibers, a method to relate whole ligament data with ligament fiber data is necessary.

Data from Pioletti [32], Robinson [34], Harner [54], Quapp [31], and Butler [27], was included in to model to establish the behavior of the whole ligaments. The data was used in comparison with split ligament fiber data from the 2D dynamic model to determine a factor that could be calculated to split the whole ligament data into fibers. Using the regression method of minimum error, f_a and f_p, the anterior and posterior forces of the ACL from the model, were used to find a coefficient that satisfied condition $f_p = a_1 f_a$ with minimum error. The minimum error led to $a_1 = \sum f_p f_a / \sum {f_a}^2$. Once factor a_1 was determined, conversion from the whole ligament force into anterior/posterior ligament fibers became possible. The factor for ACL and PCL was applied as $F_a = \frac{F}{a_1+1}$, and $F_p = \frac{F \cdot a_1}{a_1+1}$, where a_1 is the coefficient, F is the whole ligament force, a is anterior, and p is posterior.

The MCL was similar, but different, because it had three fibers. To split MCL whole ligament into fibers, the equations for $a_3 = \sum f_d f_a / \sum {f_a}^2$ and $a_4 = \sum f_o f_a / \sum {f_a}^2$ were used, where d is MCL deep, o is MCL oblique, a is MCL anterior, and a_3 and a_4 are coefficients from MCL deep and MCL oblique, respectively. Splitting of MCL deep whole ligament into MCL fibers was completed using $F_a = \frac{F}{a_3+a_4+1}$, $F_d = \frac{F \cdot a_3}{a_3+a_4+1}$, and $f_o = \frac{F \cdot a_4}{a_3+a_4+1}$, where F is force in whole fiber data, and a_3 and a_4 are factors for conversion. Splitting fibers was achieved based on the assumption that data for whole and split fibers was correct. Therefore, the overall force of fibers is interchangeable with whole ligaments using this method of conversion.

4.8 Modeling Knee Contact

4.8.1 Deformable Contact

During knee flexion and extension the bones in the joint roll and slide against one another. The bones are not directly in contact with one another, for that would wear away the bone over the thousands of daily loading cycles. A thin layer of articular cartilage between 0.1 mm and 7 mm in thickness [39] covers the rolling surfaces of the bones. Although very thin, this layer of cartilage adequately cushions the ends of the bones to prevent them from rubbing against each other within the joint. The cartilage serves as both shock absorber and lubricant, and it is essential for joint mobility. The absence and deterioration of cartilage do to wear causes painful bone-on-bone contact and can severely limit the joint's range of motion. Therefore, it is necessary to protect your cartilage and when the cartilage is worn, such as in cases of osteoarthritis, surgical repair is required.

There are two different kinds of cartilage in the knee joint: hyaline and fibrous cartilage. Hyaline cartilage (also known as articular cartilage) is the cartilage found on the surface of the femur, tibia, and patella. The primary purpose of the articular cartilage is for friction reduction in joint movement and some shock absorption. The other cartilage found is fibrous cartilage, which is what composes of the meniscus. Fibrous cartilage is very tough and its purpose in the knee is to distribute the loads between the femur and tibia throughout the bone's surface. The meniscus lies on the tibial plateau between the articular cartilage of the tibia and femur. It's C-Shape and wedged profile allow the meniscus to sit firmly on the tibia and distribute the body weight forces from the femur.

As the knee joint undergoes compressive loading from ground reaction forces and body and other external forces, the cartilage is squeezed by the bones. Therefore, the joint contact

force can be modeled as a function of the cartilage deformation. The knee is typically described in three dimensions. However, to visualize and ultimately model contact in two dimensions, one must make various assumptions. One such assumption is about the shapes of the femur and tibia in two dimensions. The surface of the femur has convex condyles with a prominence that have a far different profile in the sagittal plane than the deep notch of the intercondylar surface near the center of the femur surface. With such variances along the sagittal plane of the bones, depending on where the knee plane is "sliced," one can have different profiles for the bones. Therefore, anatomical data was used in the model from a digitized knee to simulate the shapes of the bone. Another assumption is that the bones are able to overlap, and the overlapping area and the contact force are proportional. The deformation of knee cartilage has been tested and one can see in Fig. (20), it is quadratic in force-deformation response.

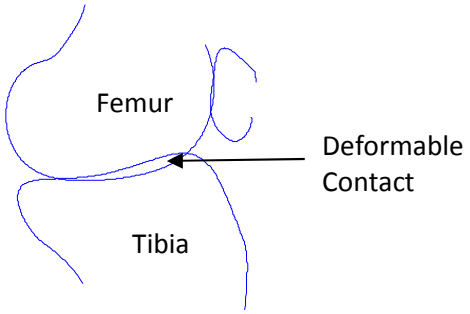

Figure 19: *Overlapping Contact Area*

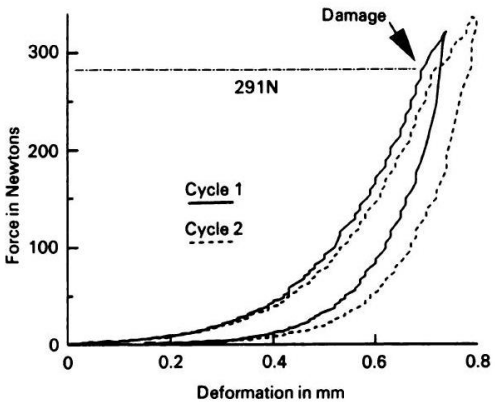

Figure 20: *Cartilage-Loading Mechanical Behavior*

4.8.2 Calculation of Contact Area

The calculation of the area of the deformable contact is given next. When there are two curves bounded by the same endpoints, the area between the curves is found by integrating the curves and subtracting the bottom curve's area from the top curve's area. A Matlab numerical integrator called *trapz* is used. Function *trapz* is a trapezoidal integrator that approximates the integral using the trapezoidal method shown in Fig. (21).

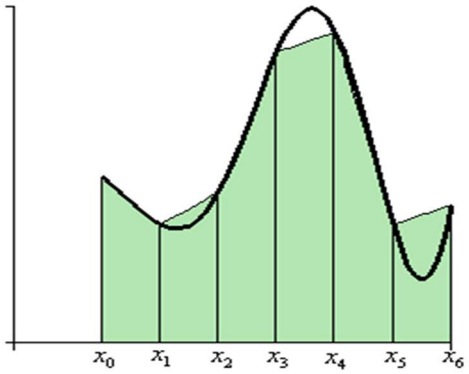

Figure 21: *Trapezoidal Integration*

In order to use *trapz*, the curves being integrated must be linearly spaced, which is not the case with the digitized curves. There are actually several initial constraints for the digitized 2D curves when it comes to contact modeling. First of all, the contact only occurs over a small portion of the total points of the femur and tibia curves. To get a sufficient number of points in the contact overlap area for *trapz* accuracy, there would have to be a large number of points defining the bone curves. The points on the bone curves are not linearly spaced. These curves are described by parametric 10th degree polynomials. Because the curves are complex with convex, concave, and varying levels of curvature, there is no simple way to linearly space the curves. In the following discussion, a method is explained which finds the *trapz* integral of the contact overlap area and the unit vectors associated with the contact force.

4.8.3 Intersection Points and Finding the Contact Area

The first step in finding the contact area is to identify the intersection points of the two curves that are sharing a contact overlap. The intersection points of two curves are found using a Matlab file exchange script titled, "Fast and Robust Curve Intersections," by Douglas Schwarz. Coordinate points of bone plots at an instantaneous position are fed to the *Intersections* function, and the solution returns the specific coordinates of any intersecting points. The code has been rigorously tested and has so far been accurate in every single test encountered regardless of the complexity of the curve positions. The solution of *Intersections* when an intersection pair is found is shown in Eq. (42)

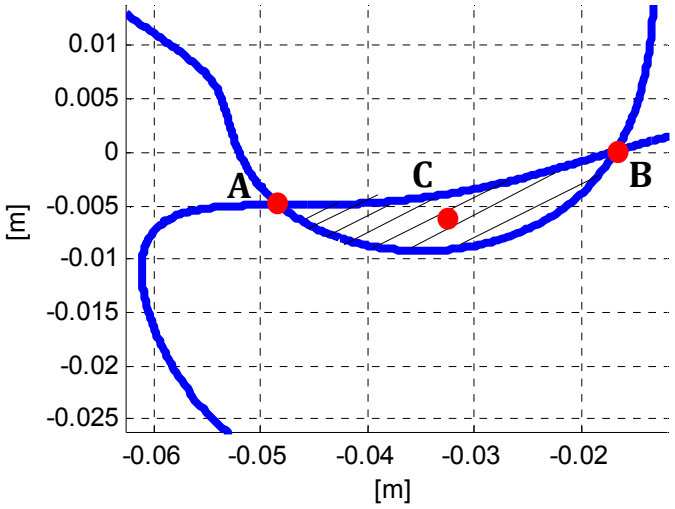

Figure 22: *Contact Overlap Area. Intersections labeled A and B. C is the Center of Mass of the Unit Vectors of the Contact Force.*

$$[Intr.1 \quad Intr.2] = \begin{bmatrix} x_{intr1} & x_{intr2} \\ y_{intr1} & y_{intr2} \end{bmatrix} \tag{42}$$

The function *Intersections* returns the exact positions along the bone curves where the intersections occur. Since each curve is composed of a thousand individual coordinate *x*-*y* pairs, the intersection will very rarely land on a pair of points already defined by the curve. The intersection point that is exactly where a line connecting the points of the femur crosses with a

line connecting the points of the tibia curve, lands somewhere in-between points of the tibia and femur. Consequently, the intersections function results in the intersection coordinates being precise values that are not a match with any of the 1000 coordinate pairs of either curve. The intersection points are rounded to the nearest coordinate pair by an error minimization loop and the error is negligibly small. The *Intersections* function also reveals the position of the intersecting coordinates in the curve array. For example, if there are 1000 points along the tibia and the intersections of contact occur at points 624.245 and 651.502, then the intersection coordinates will be the 624^{th} and 652^{nd} elements of the tibia array.

$$x1r = XfR(1, iF2{:}\, if1) \tag{43}$$

In this example, there are 652-624 +1= 29 points of contact that are not linearly spaced for the tibia. For this same example the femur happens to have 23 points of contact between the same two intersection points. The points will be used for creating a new vector defining the contacting curve, Eq. (43). To increase the accuracy of this section of the model, a highly refined bone mesh is used as a reference for the intersection pair so that negligent rounding is done in the model. The highly refined mesh is the bone curves composed of 100,000 points, and when *Intersections* is used, it is on a coarse mesh with 400 points. Using the approximate intersection from the coarse mesh, the nearest point in to the intersection point in the 100,000 point mesh is taken to get good accuracy in the model contact, and without slowing down the simulation. Mathematically, this is done using the sum of least squares regression in *Contact.*

These coordinates, found using the highly defined mesh, are not linearly spaced and only represent small portions of tibia and femur bone curves. The coordinates are in a global (*X,Y*) coordinate system, so to use *trapz*, they need to be linearly spaced along an axis. To solve this problem, a local coordinate system is considered with the *p*-axis connecting the intersection

points, with the sense from intersection 1 on tibia to intersection 2 on tibia. Once this axis was chosen, the angle between the intersecting line and the global X-axis was found. This angle (φ), allows the rotation of the contact coordinate points into a new localized coordinate system. The curves are translated into a new coordinate system, but the curve points must be linearly spaced for *trapz* to be accurate. To achieve linear spacing, polynomial equations that define this section of the contact curves are then solved for. The Matlab function that can perform this task is *polyfit*.

$$[QSCOFE, ss1] = polyfit(p1s, q1s, degree) \tag{44}$$

Polyfit is a polynomial curve fitting function that uses the least-squares approach to find a curve equation at a set degree, Eq. (44). For the level of curvature that is occurring in the 1-7 mm range of contact, the curves can accurately be defined with an8^{th} degree polynomial with a few exceptions, Fig. (23).By deciding to use an 8^{th}degree polynomial, an assumption must be made, which is that any contact section with less than 9 points of contact will be assumed to be no contact. The reason for this is because in order for the 8^{th} degree polynomial equation to be conditioned, it must have at least 9 input points. Nine points or less is considered negligible because the contact area will create a very small force below 5N. A consequence of this is that contact may create a sharp initial step, with a jump between 0 and 5N in size. However this has been tested and it shows no significant impact. Additionally, the way the code has been designed the model will simulate *polyfit* and find the norm of the residuals for the curve. This norm must meet the criteria of being less than 0.001 (the closer to zero the more accurate). Consequently, the contact function will increase the degree of the polynomial if sufficient accuracy is not obtained in the initial calculation. The use of a *while* loop guarantees that the *polyfit* will be

fitted to below 0.001 norm, with a cap of 10 degrees to prevent an infinite loop from occurring in case less than 0.001 norm cannot be obtained.

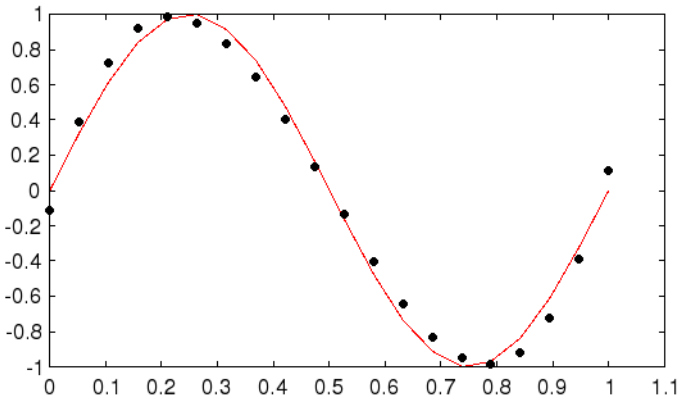

***Figure 23**: Polynomial Curve Fitting*

Matlab function *polyfit* finds the curve coefficients, which are then transformed to a new, local array of points using *polyval*. The *polyval* function automatically generates a new curve position vector when given the coefficients. In the following example from the code, p1r is the local *p*-axis for the rotated contact curve coordinate system. The local contact curve is rotated by angle, φ, and Eqs. (45a) and (45b) are used to transform the x-y coordinates (*x1r, y1r*) to the new *p-q* coordinate system (*p1r,q1r*).

$$p1r = \cos\varphi \cdot x1r + \sin\varphi \cdot y1r \tag{45a}$$

$$q1r = -\sin\varphi \cdot x1r + \cos\varphi \cdot y1r \tag{45b}$$

The reason *polyfit* was implemented in the first place was to have the exact curve equation for the contact curve vs. a linearly spaced axis - for the *trapz* function. To get the linearly spaced curve, the *linspace* function is used to create an array of points linearly spaced along the newly created local *p-q* coordinate system (localized intersection points). The *p-q* coordinate system is a system that is rotated with respect to the global system in order to have the *p*-axis along the line connecting the intersection points of the contact curves. The *q*-axis is

perpendicular to the *p*-axis in 2D. The *linspace* array is used as the local *p*-coordinate (*pfr*) and the *polyfit* equation is used to solve the local *q*-coordinates (*qfr*) of the curve. QCOFE (Q-Coefficients Femur) is the array of local femoral coefficients resulting from *polyfit* on the contact curve (*p1r,q1r*). The terms *q1r*, *diff* and *min*, are used to shift and rotate the local contact curves so they have an origin at zero to help with the integration.

$$qfr = q1r_{diff} \cdot QCOFE + q1r_{min} + q1r(1) \tag{46}$$

Once data points for the local *p* and *q*-coordinate system are obtained, the *trapz* function is used to find the area between the tibia and femur curves of contact. The area difference is calculated by subtraction, and finds the total area of contact between bones. The contact force is proportional to the area and is found using the equation: *F=kA*.

In order to obtain the local coordinate curves accurately for *polyfit*, standardization, Eq. (47), was performed on the section of the contact area that was between the intersecting points. The standardization Eq. (47) converts all local *p*- and *q*-coordinates, Eq. (48), to be between 0 and 1 to obtain accurate curves from *polyfit*. These points were standardized by Eq. (47).

$$X(n) = \frac{X(n) - X_{min}}{X_{max} - X_{min}} \tag{47}$$

To un-standardize the points after all vector operations are performed, the equation is simply undone by multiplying by the denominator of Eq. (47) then adding X_{min}. The standardization conditions the curve and is critical to an accurate model. In Fig. (19), the curves of the tibia and femur intersect. As seen in Fig. (22), the intersecting points A and B would be connected by the *p*-axis which is used as the local coordinate axis for contact.

Following the aforementioned steps, the centroid of the contact area is found as follows. It is assumed that the contact force is perpendicular to the intersection line and passes through the centroid of the contact area. The local *p*-coordinate for centroid, as shown in Eq. (49) and

Fig. (24), is used to find the ratio of points of contact. Therefore, if the centroid is 0.45, and there are 100 points of contact, the coordinates of the 45th point of the contact on the bone are used as the location on the bone surface where the force will be applied. Numerical simulations demonstrated this to be a consistent assumption.

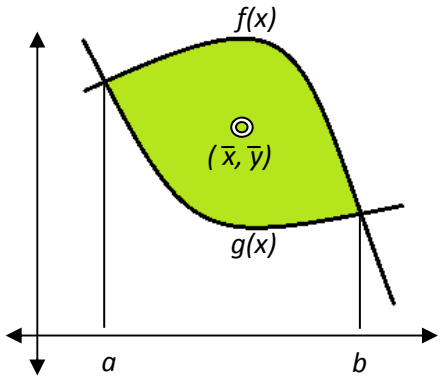

***Figure 24**: Centroid of an Area Between Two Curves*

$$Centroid_p = \frac{\int_a^b \xi(f-g)d\xi}{\int_a^b (f-g)d\xi} \tag{49}$$

This is how patello-femoral and tibio-femoral contact forces are found as vectors in the global coordinate system. With the normal vectors and force values calculated, the moment of the contact force is found just as it was found for ligaments. These calculations are repeated at each position and for the different points of contact in the model. As a result, the contact forces and moments can then be summed in bones to find the overall resultant forces and moments acting on the bone's centers of mass.

CHAPTER V

PROXIMAL-DISTAL VIBRATION OF TIBIA TEST

5.1 Introduction

A new test for detecting ligament deficiencies is proposed. This is a proximal-distal forced vibration of tibia test that could be replicated in the laboratory environment, and can be used to detect early ligament deficiencies in the knee. This test is best described as the "nervous leg" test from sitting position. The leg is at 90ºflexion angle. Tibia oscillates up and down from an actuation at the foot level, for simplification, at the ankle joint. The femoral Y-coordinate of the center of mass frequency response to these oscillations is investigated. The model includes viscoelastic ligaments, and investigates different levels of deficiencies of knee ligaments.

5.2 Assumptions

Several assumptions were made to allow us to perform this forced vibration test in our model. Assumptions made for this straightforward 2D tibio-femoral anatomical knee model experiment for proximal-distal (vertical) tibial forced vibration test are as follows:

1) The motion of tibia is due to proximal-distal (vertical) harmonic excitation at the ankle level. Therefore, minimal flexion-extension motion is present.

2) The horizontal motion (along the *x*-axis) of the ankle is negligible, since only small vertical (*y*-axis) forces are used. This constraint gives tibia a piston-like behavior.

3) The contact force between tibia and femur during the test is not negligible. There will be contact due to femoral inertia.

4) The articular contact is modeled as deformable contact in this work.

5) The elastic properties of the ligaments are nonlinear [20].

6) The friction in the knee joint is neglected. It is well known that the level of articular contact friction in synovial joints is not significant [13].

7) The internal-external rotation and varus-valgus are not significant in this test. The screw-home mechanism [9] is negligible since no large flexion-extension motion occurs.

8) The ligaments are treated both as elastic or viscoelastic in order to investigate the difference.

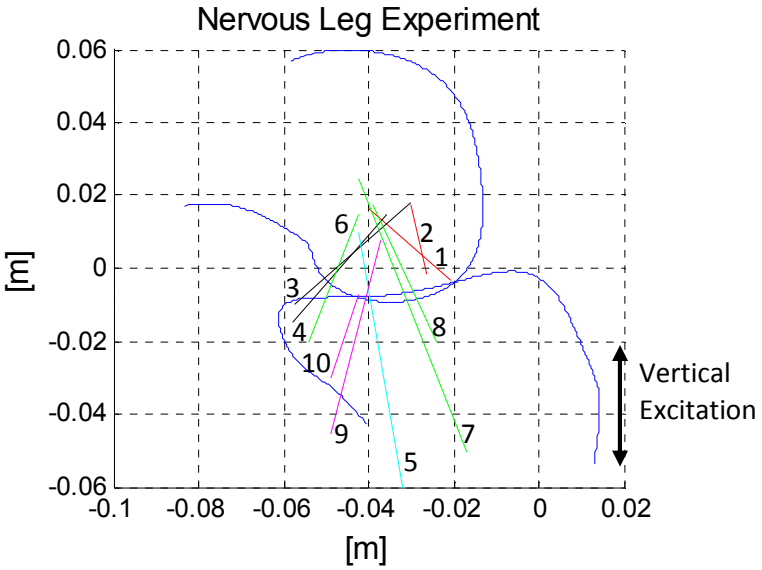

Figure 25: *Initial Sitting Position Prior to Lower Leg Excitation. An Open-Chain Exercise; x-Axis Horizontal and y-Axis Vertical.*

The DAE system of first order differential equations describing the "nervous leg" motion, proximal-distal vibration of tibia is as described in Eqs. (51) and (52). Eq. (52) is the differential algebraic equation set describing the motion of the system, and contains three algebraic

constraints. The first two constraints are to pin the femur at the hip so that it simulates femoral oscillatory motion of a person who is sitting down. This is done by setting the *x* and *y* velocities of the femur at the hip joint to zero at all times. The third constraint is a zero *x* velocity constraint at the ankle to keep the foot from swinging front and back.

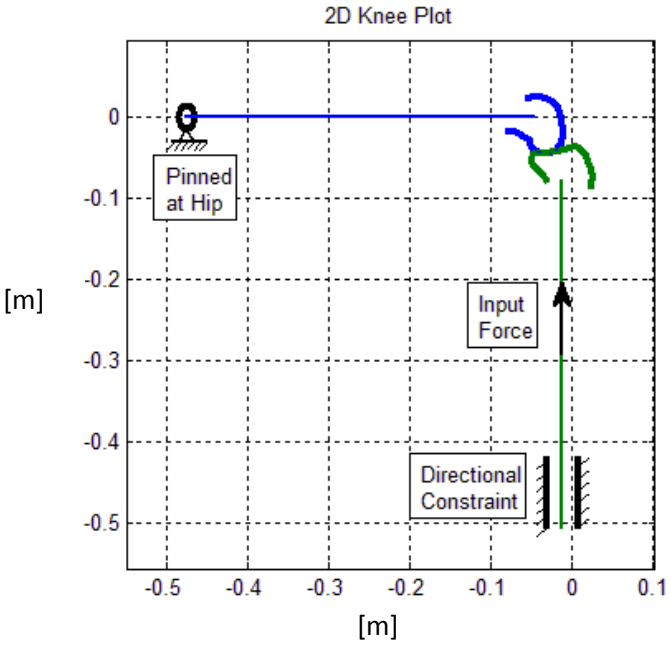

Figure 26: *Diagram of Experiment, Initial Position*

5.3 Differential Equations of Motion

The variables x_1 and x_2 are displacement and velocity, respectively. The dot above *x* represents the derivative with respect to time. Therefore, $x_1 = x(t);\ x_2 = \dot{x}(t)$.

For the first 12 entries in the system in Eq. (51) the variables with 01 represent the femur, and 02 the tibia; *X* and *Y* are global coordinates of centers of mass. *Vx* is the velocity of the center of mass along *X* axis, θ's are angles of the bones with respect to the global coordinate system and ω's are their corresponding angular velocities. ε is the strain and $\dot{\varepsilon}$ is strain rate for ligaments fibers 1-10, as numbered in Table 5.

Where m is the mass of tibia, ΣF_{lx} is the sum of ligament forces in the x direction, and f is the frequency of actuation, $\Omega = 2\pi f$ .The ligamentous elastic forces are nonlinear as follows:

$$F_l = \begin{cases} 0 & \varepsilon \le 0 \\ kq\left(L - L_0\right)^2 & 0 \le \varepsilon \le 2\varepsilon_0 \\ kl\left(L - \left(1+\varepsilon_0\right)L_0\right) & 2\varepsilon_0 \le \varepsilon \end{cases} \tag{50}$$

Where kq is the elastic constant for the quadratic part of the force displacement curve of the ligaments, kl is the elastic constant of the linear part, and ε is the strain in the ligament. The threshold strain level ε_0, is a value calculated by setting the last two equations of Eq. (50) as equal to each other and solving for ε_0 [27]. Eq. (50) does not account for the strain rate effects (viscoelastic effect).Once the strain rate has been identified, the ligament viscous force is calculated and included in the system of equations. This results in a realistic force of the ligament at its current strain and strain rate.

$$
\begin{aligned}
X(1) &= X_{01} \\
X(2) &= V_{01x} \\
X(3) &= Y_{01} \\
X(4) &= V_{01y} \\
X(5) &= \theta_1 \\
X(6) &= \omega_1 \\
X(7) &= X_{02} \\
X(8) &= V_{02x} \\
X(9) &= Y_{02} \\
X(10) &= V_{02y} \\
X(11) &= \theta_2 \\
X(12) &= \omega_2 \\
X(13) &= \varepsilon_{01} \\
X(14) &= \dot{\varepsilon}_{01} \\
X(15) &= \varepsilon_{02} \\
X(16) &= \dot{\varepsilon}_{02} \\
X(17) &= \varepsilon_{03} \\
X(18) &= \dot{\varepsilon}_{03} \\
X(19) &= \varepsilon_{04} \\
X(20) &= \dot{\varepsilon}_{04} \\
X(21) &= \varepsilon_{05} \\
X(22) &= \dot{\varepsilon}_{05} \\
X(23) &= \varepsilon_{06} \\
X(24) &= \dot{\varepsilon}_{06} \\
X(25) &= \varepsilon_{07} \\
X(26) &= \dot{\varepsilon}_{07} \\
X(27) &= \varepsilon_{08} \\
X(28) &= \dot{\varepsilon}_{08} \\
X(29) &= \varepsilon_{09} \\
X(30) &= \dot{\varepsilon}_{09} \\
X(31) &= \varepsilon_{10} \\
X(32) &= \dot{\varepsilon}_{10}
\end{aligned}
\tag{51}
$$

$$
\begin{cases}
\dot{x}_1 = x_2 \\
0 = x_2 - \dfrac{l_f}{2} x_6 \cos(x_5) \\
\dot{x}_3 = x_4 \\
0 = x_4 - \dfrac{l_f}{2} x_6 \sin(x_5) \\
\dot{x}_5 = x_6 \\
\dot{x}_6 = \dfrac{1}{I_{f/hip}} \left(\sum M_{f/hip} + \dfrac{l_f}{2} \left(\sum F_{fy} \sin(x_5) + \sum F_{fx} \sin(x_5) \right) \right) \\
\dot{x}_7 = x_8 \\
0 = x_8 + \dfrac{l_t}{2} x_{12} \cos(x_{11}) \\
\dot{x}_9 = x_{10} \\
\dot{x}_{10} = x_{10} + \dfrac{l_t}{2} x_{12} \sin(x_{11}) + Y_{ankle}\, \omega \sin(\omega t) \\
\dot{x}_{11} = x_{12} \\
\dot{x}_{12} - \dfrac{m_t l_t}{2 I_G} [(\dot{x}_{10} \sin(x_{11}) +] = \dfrac{1}{I_{t/o}} \left(\sum M_{Ankle} \right) \\
\dot{x}_{13} = x_{14} \\
0 = x_{14} - \dot{L}(1) / SL(1) \\
\dot{x}_{15} = x_{16} \\
0 = x_{16} - \dot{L}(2) / SL(2) \\
\dot{x}_{17} = x_{18} \\
0 = x_{18} - \dot{L}(3) / SL(3) \\
\dot{x}_{19} = x_{20} \\
0 = x_{20} - \dot{L}(4) / SL(4) \\
\dot{x}_{21} = x_{22} \\
0 = x_{22} - \dot{L}(5) / SL(5) \\
\dot{x}_{23} = x_{24} \\
0 = x_{24} - \dot{L}(6) / SL(6) \\
\dot{x}_{25} = x_{26} \\
0 = x_{26} - \dot{L}(7) / SL(7) \\
\dot{x}_{27} = x_{28} \\
0 = x_{28} - \dot{L}(8) / SL(8) \\
\dot{x}_{29} = x_{30} \\
0 = x_{30} - \dot{L}(9) / SL(9) \\
\dot{x}_{31} = x_{32} \\
0 = x_{32} - \dot{L}(10) / SL(10)
\end{cases}
\tag{52}
$$

5.4 Description of the Test

In the "nervous leg" test the femur is pinned at the hip, and the ankle is constrained from lateral displacement. However the model does not include a floor restraint at the foot. A forced oscillation is applied at the ankle. Therefore, for this experiment, the foot vibrates at various frequencies, and the amplitude-frequency response of the *Y*-coordinate of the center of mass of femur is investigated.

A numerical simulation was conducted to validate the ground reaction force while the leg is at rest. The static GRF force based on the mass of our system should be 78.5 N, which was in agreement with analytical calculations. A new simulation was conducted for finding the equilibrium position of the knee joint. Both the ankle and hip were pinned. The model simulation determined the equilibrium position, which is used as initial position for the tests.

5.5 Frequency Response for Ligament Deficiency Detection

The proposed testing exercise allows for investigating the ACL and PCL ligaments contribution to the knee ligament structure at various frequencies of excitation. The algorithm used to solve the DAE system was *ode15s* (Solve stiff differential equations and DAEs; variable order method) in Matlab. For the integration of the contact curves, the *trapz* function was used in Matlab. Function *trapz* computes an approximation of the integral using the trapezoidal method. The results of the tests with a forced oscillation (vibration) at the ankle are reported using the relative amplitude of the femur in the *Y*-direction with respect to the amplitude of the ankle. It is assumed that the ankle oscillation is in the vertical direction and the *x*-axis ankle motion is zero. The frequency of excitation at the ankle was between 5 Hz and 40 Hz. The amplitudes of excitation of the ankle were calculated in such a way that the actuating force stays constant. The

limit of 40 Hz is chosen intentionally, because when increasing the frequency above 40 Hz, the amplitudes become too small to be measured. As shown in Table 6, at 40 Hz the amplitude is already at 0.39 mm, and this is a small value. Values smaller than this, will be beyond the limits of this model since it does not account for the soft tissue of the foot.

In Fig. (27), a typical solution to the model is shown for elastic ligament model and for viscoelastic ligament model. The viscoelastic ligament model, due to viscous effects on the system, results in a more stable lower amplitude motion (blue color). The green color shows the elastic ligament model. Large amplitudes of the elastic model result when compared to the viscoelastic model.

Table 6: Amplitudes to maintain 5N force at varying frequencies

f (Hz)	Amplitude(m)
5	0.025
10	0.00625
15	0.002778
20	0.001563
22.5	0.001235
25	0.001
27.5	0.000826
30	0.000694
32.5	0.000592
35	0.00051
37.5	0.000444
40	0.000391

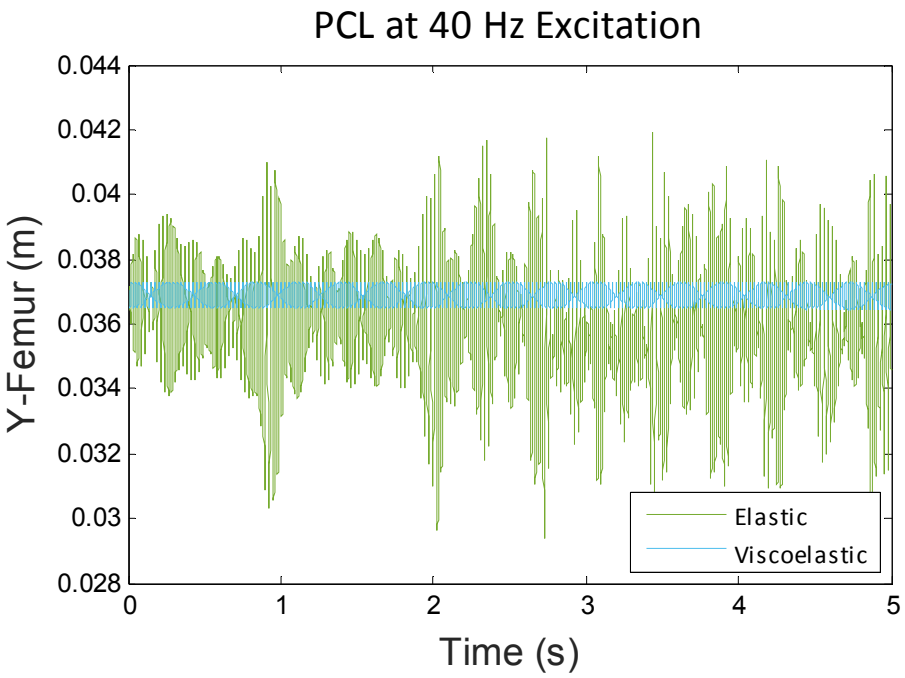

Figure 27: *Time Response for PCL Deficiency at 40 Hz*

The ratio of the *Y*-amplitude of the center of mass of femur to the *Y*-amplitude of the ankle is called the relative amplitude. It is plotted versus frequency results from multiple simulations. Results are shown in Figs. (28) and (29).

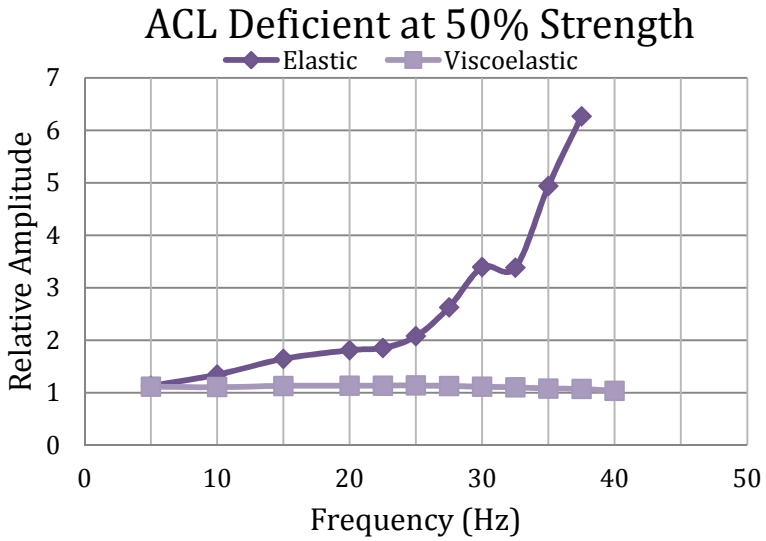

Figure 28: *Frequency-Amplitude Response of ACL Deficient Knee in the Case of Elastic and Viscoelastic Models*

5.5.1 Elastic vs Viscoelastic ACL Deficient Knees

Fig. (28) is the frequency response of the model with the ACL deficiency tested at 50% ACL strength, while all the other ligaments retain normal strength. In other words, the elastic force in the ACL ligament is 50% of the normal ligament force of a healthy knee ACL. This could represent an ACL fiber that has undergone laxity and creep over the years, meaning that relative amplitude of the frequency response of the viscoelastic ligament model of the "nervous leg" is not affected by the frequency of excitation. Conversely, the frequency response of the elastic ligament model shows a resonance around 40 N.

One can conclude that for high-speed tests, such as the one in this section, the ligament viscoelastic model is necessary, as the elastic model erroneously predicting unrealistic resonances (behavior).

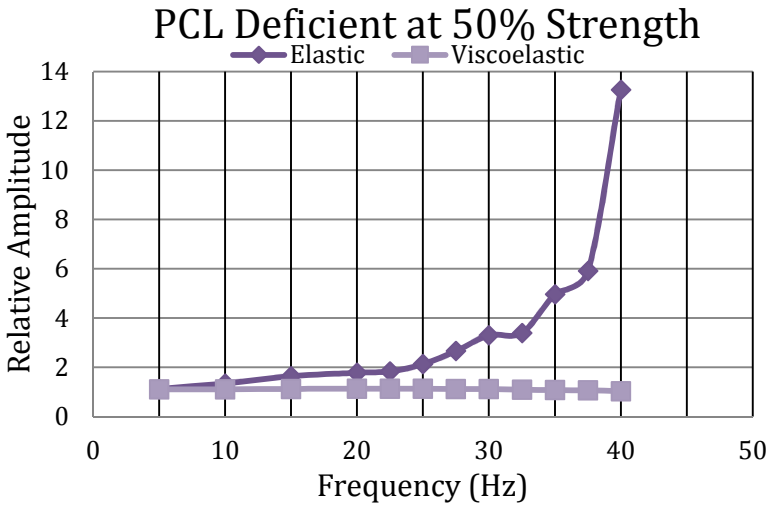

Figure 29: *Frequency-Amplitude Response of PCL Deficient Knee in the Case of Elastic and Viscoelastic Models*

5.5.2 Elastic vs Viscoelastic PCL Deficient Knees

Fig. (29) is the frequency response of the "nervous leg" test under the condition that PCL is deficient in both elastic and viscoelastic cases. In the case of deficiency, PCL has only 50% of the force of a healthy PCL, while all the other ligaments retain normal strength. Fig. (29) resembles the behavior of Fig. (28). Again, the ligament viscoelastic model is necessary since the elastic model erroneously predicts unrealistic resonances (behavior).

5.5.3 Viscoelastic Model – Normal vs ACL Deficient Knees

In this section only the viscoelastic ligament model is used. ACL variable strength effect on the frequency response is investigated. This is done by reducing the strength of the ACL to the extent that the ligament is removed altogether from the model. The intent of this exercise is to see if any ligament tears can be detected while being non-intrusive to the patient.

The ACL could not be tested in a fully ruptured condition because the knee in the model would lose all force resistance for the anterior motion of tibia. In this model patella and the patellar tendon that could prevent this are not included in this model. This might be a limitation of this work. To circumvent this limitation for the current exercise and assumption was made that the ACL ligament would be tested with only 5% of its strength and also at 10% of its strength to simulate a rupture without completely removing the ligament from the model during the test. The benefit of this condition is that it gets very close to a rupture condition, and the model would still have tibia anterior displacement resistance.

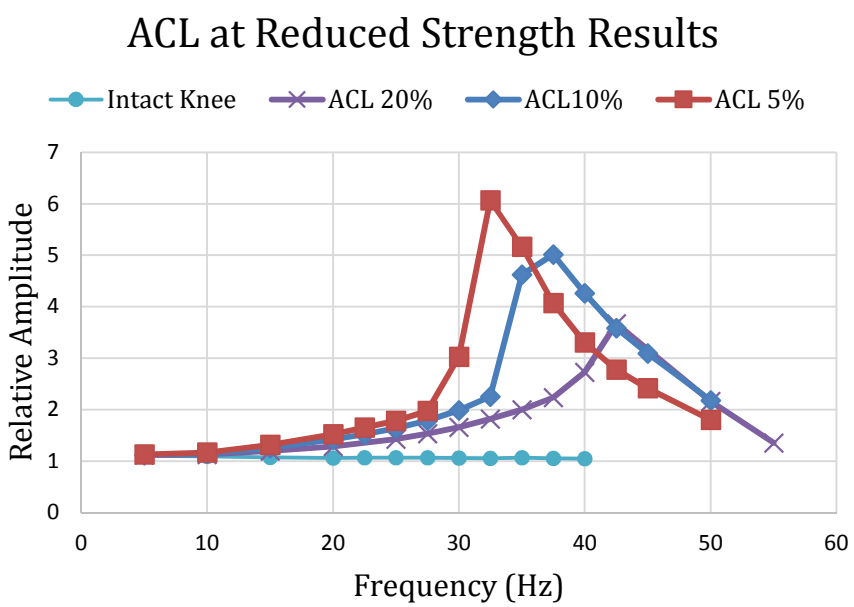

Figure 30: *Frequency-Amplitude Response for ACL Deficient Knees with Lower ACL Ligament Strength to Simulate a Rupture, Viscoelastic Model*

The results of the testing for 5% and 10% ligament strength of the ACL, in Fig.(30),show that as the ACL strength is reduced, the natural frequency (resonant frequency) of the system is shifted from 37 Hz for 10% strength to approximately 32 Hz for 5% strength. Meanwhile, the peak amplitude increases. Therefore, if the knee had ACL damage, with the proposed "nervous leg" test the damage can be detected (in the resonance zone the amplitudes of the femoral center of mass exceed the expected amplitude in Table 6). Based on the frequency response one could find if the ACL is damaged. The resonant frequency is shifted below 40 Hz.

5.5.4 Viscoelastic Model – Normal vs PCL Deficient Knees

Here only the viscoelastic ligament model is used. The PCL was tested for the rupture condition and compared to an intact (normal) knee. The PCL testing when the ligament is torn can be analyzed in Fig. (31).

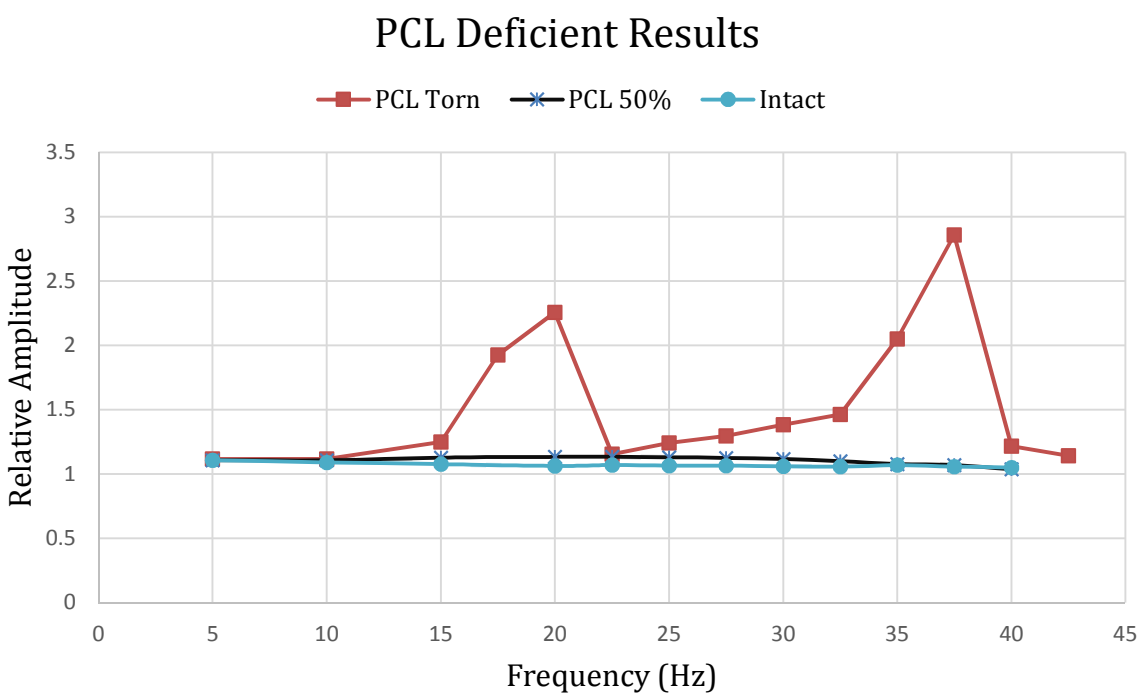

Figure 31:*Frequency-Amplitude Response for PCL Deficient Knees with 50% Strength and Torn PCL Ligament, Viscoelastic Model*

The knee with intact ligaments is used as the reference point in this test. Fig. (31) shows that at 50% strength of the PCL, the frequency begins to have a slight effect on the response in comparison to the intact knee. The black curve begins to separate from the blue intact curve. The amplitudes in the case of 50% PCL and Intact knee are relatively small. One can conclude that these frequencies are away from the natural frequencies of the system, which should be above 40 Hz. However, the orange line shows the response when PCL is ruptured, and one can notice that the response is very different. When a ruptured PCL is tested at 20 Hz, or above 35 Hz, two resonant resonance frequencies are found. This is a significant result since one can experimentally test a knee with a small oscillating force at the ankle at 20 Hz, and conclude if there is significant damage in the ligament without using an MRI.

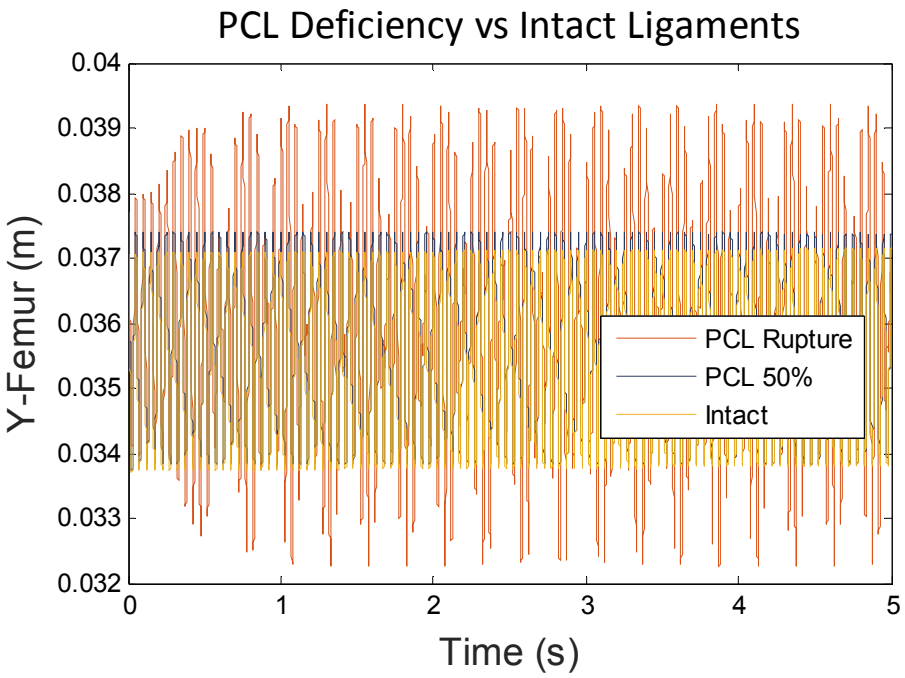

Figure 32: *Time Response at 20 Hz of PCL Deficient Knees*

Delving further into the results of Fig. (31), in Fig. (32) one can see the actual time response of the knee model at 20 Hz. A beating phenomenon is seen at this frequency when the PCL is torn, and this is indicative of being near a natural frequency. This finding for the ruptured ligament needs to be laboratory tested, and at 20 Hz (using Table 6). If the results hold true in the lab, then the center of mass of femur would theoretically vibrate vertically at amplitudes of 3 mm when undergoing the test.

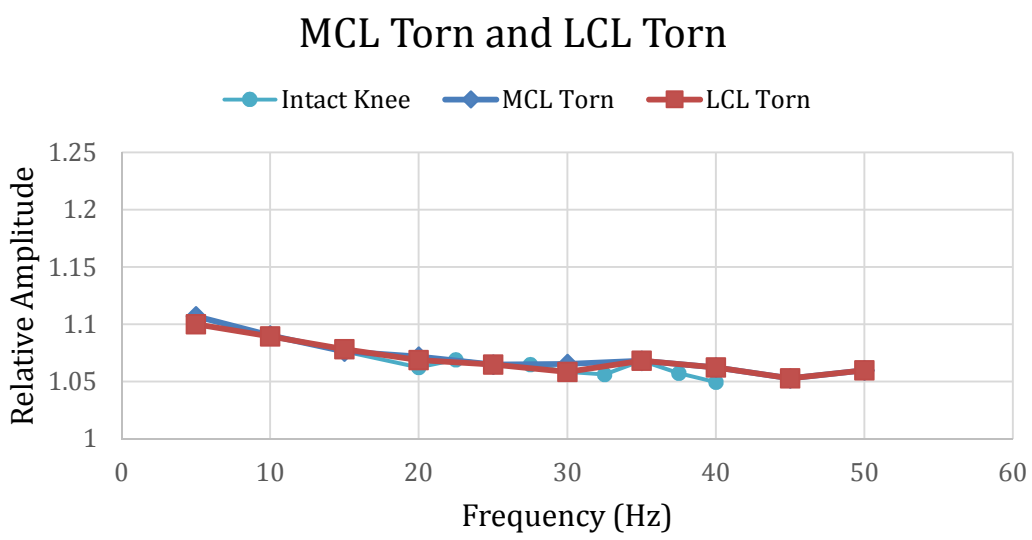

Figure 33: *Frequency Response in the Case of MCL Torn and LCL Torn*

5.5.5 Viscoelastic Model – Normal vs LCL or MCL Deficient Knees

In this section only the viscoelastic ligament model is used. "Nervous leg" simulations were conducted with deficient (torn) LCL or deficient (torn) MCL. Fig. (33) shows that LCL and MCL have a small effect on the knee below 40 Hz in this type of exercise. Therefore, these deficiencies cannot be detected using this type of exercise under 40 Hz.

5.6 Discussion and Conclusions

We investigated the frequency response of the human leg from a sitting position under a proximal-distal (vertical) vibration on tibia with the purpose of characterizing deficient knees. A two dimensional model describing the three degree of freedom motion of the system comprised of femur, tibia, knee ligamentous structure and knee articular cartilage has been used to investigate the behavior of the knee at various forcing frequencies. A mathematical model consisting of a DAE system of thirty-two equations has been developed. The DAE system has been integrated using Matlab. The results reported in this work showed that for ACL almost

ruptured knees, a natural frequency exists at 32 Hz. As for the PCL ruptured knees, a natural frequency of the leg exists in frequencies around 20 Hz. Fig. (31) shows a comparison between intact knee and PCL deficient knee at 20 Hz frequency of excitation and shows that it may be feasible for PCL rupture testing using an oscillating force of 5N at the tibia. The MCL and LCL fibers do not show any significant effect when deficient in the proposed test. This is expected, since the MCL and LCL are not the primary restraints in the sagittal plane.

One can notice that the relative amplitude of the PCL deficient knees is larger than the one of intact knees. Therefore, the lack of PCL lowers the stiffness of the knee and leads to two resonant frequencies below 40 Hz, Fig. (31).The frequency response for no ACL case also may be predicted by using the "nervous leg" test. This work clearly demonstrates that altering the ligamentous structure results in natural frequencies shifting to lower values and increased relative amplitudes of vibration. This can be tested *in vivo*. Therefore, this testing exercise can predict changes in the elastic structure of the knee due to ligament deficiencies.

CHAPTER VI

KNEE EXTENSION EXERCISE

6.1 Introduction

To validate the model of this work, a common exercise is simulated, namely the knee extension exercise from a sitting position. It is shown afterwards that the knee model predictions are consistent with results reported in literature. The journal article with a similar model, albeit in three dimensions, was the model of Caruntu and Hefzy [4].

6.2 Assumptions

Several assumptions were made to perform the knee extension exercise, and they are as follows:

1) The patellar tendon was included in the model as a viscoelastic structure. Similar viscoelastic properties to PCL anterior (the stiffest ligament in the model, because patellar tendon strain rate data was limited) were considered for the patellar tendon.
2) The patello-femoral contact cartilage has the same stiffness coefficient as the tibio-femoral contact cartilage.
3) Patello-femoral contact is calculated using a deformable contact area, identical to tibio-femoral contact.
4) Data smoothing (*rloess* function in Matlab) is used for the predicted results.
5) The quadriceps force considered for simulations is a function of flexion angle [4].

6.3 Description of the Knee Extension Exercise

The 90°knee extension from sitting position experiment begins with the knee at a 90 degree angle, Fig. (34). The femur is fixed and tibia and patella go into extension due to actuation from the quadriceps muscle. The quadriceps muscle is connected to patella through the quadriceps tendon, which is attached to patellar basis. Patella transfers the force from the quadriceps tendon to the patellar tendon, which connects patella and tibia. The insertion points of the patellar tendon are apex on patella and tibial tuberosity on tibia. The patellar tendon pulls the tibia into an extension motion rolling along the femoral bone.

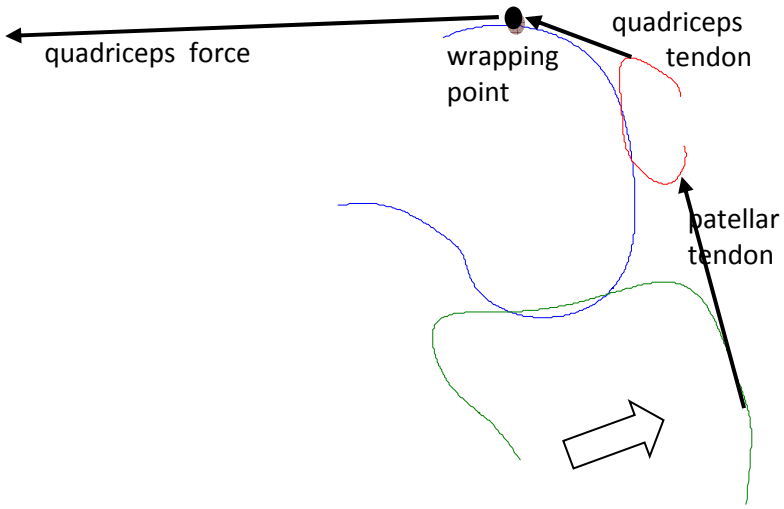

Figure 34: *Knee Extension Exercise*

In Fig. (34), the knee is in the initial position that was found by solving for system equilibrium. The starting position is very important to reduce noise in the final results. Eqs. (51) hold for the knee extension exercise with the following changes: 1) another 6 first-order differential equations describing the motion of patella are added, 2) another two equations describing the viscoelastic patellar tendon (treated as a viscoelastic ligament) are added, 3) the

patellar tendon force is included in the tibial equations, 4) the patellar contact force is included in the femoral equations, 5) the accelerations of femur and its initial velocities are zero since femur is at rest during the knee extension exercise, and 6) all the dynamics equations are Newton and Euler equations of motion.

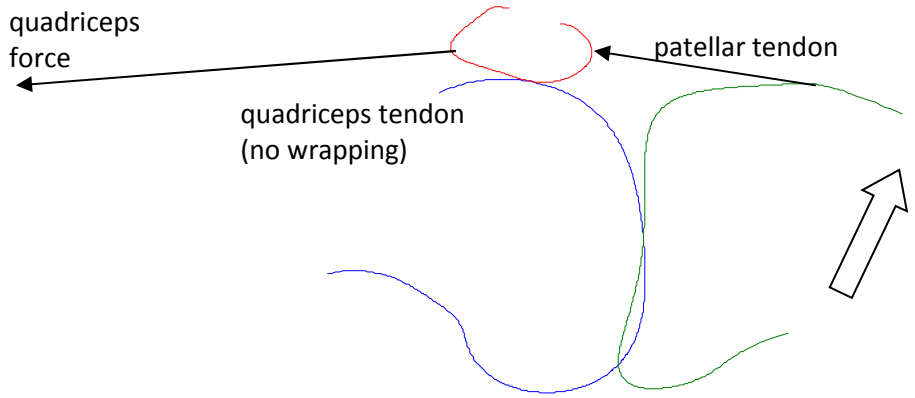

Figure 35: *Knee at Full Extension.*

At the position in Fig. (35), the knee has reached the full extension. The patella is used as a lever arm to lift the tibia from the initial resting position to the full extension.

6.4 Knee Extension Exercise Results

The quadriceps force applied to the knee for the knee extension exercise is shown in Fig. (36).The force is based on the Caruntu-Hefzy anatomical model [4] where a similar force was used for the knee extension exercise. Test results from this work for the knee extension exercise include noise in the data, due to the lack of a damping in the patella-femoral contact. To mitigate this, an equilibrium position was found for the sitting position with the ankle and hip pinned. After solving for the equilibrium position, the knee was tested and although the noise reduced significantly, some noise was still there. Consequently, local regression (filter) using weighted linear least squares and a 2^{nd} degree polynomial model was applied to the model

through the *rloess* function in Matlab. It is essentially a robust version of '*loess*' that assigns lower weight to outliers in the regression. The method assigns zero weight to data outside six mean absolute deviations. Using a coefficient for *rloess* of 0.3, the output data is filtered as shown in Figs. (37-41).

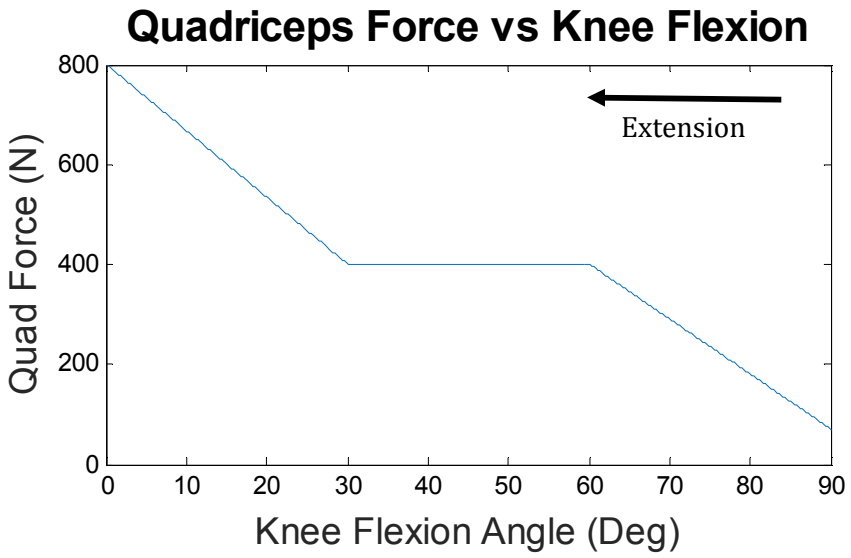

Figure 36: *Quadriceps Force vs Knee Flexion Angle for Knee Extension Exercise*

6.4.1 Patellar Flexion Angle

The knee extension exercise started from the position shown in Fig. (34). As the knee is extended, the relationship between the patellar flexion angle and knee flexion angle can be seen in Fig. (37). This is in good agreement with Ref. [4].

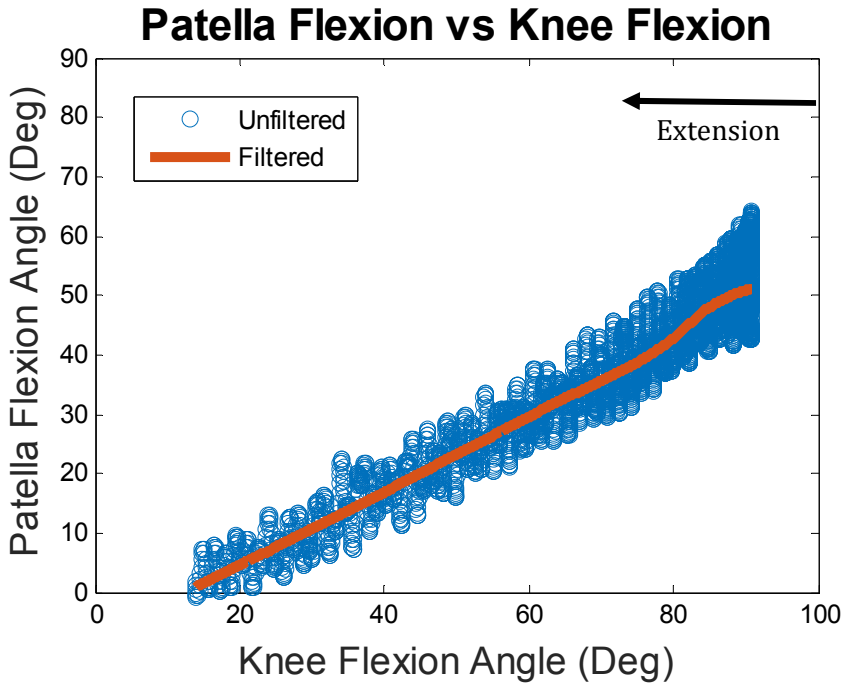

Figure 37: *Patella Flexion Angle vs Knee Flexion Angle for Knee Extension Exercise*

6.4.2 ACL Forces during Knee Extension

Figure (39) shows the forces in the ACL fibers during the knee extension exercise. The range of forces in the fibers is similar to Ref. [4]. This is a good agreement. However, the anterior and posterior ACL fibers show forces that have different patterns than Ref. [4], which reports a 3D knee mode. The patterns might be different because some of the force components could be influenced by internal-external rotation, which cannot be modeled in the sagittal plane. Additionally, the ligaments used in this work are based on the Shelburne [3].

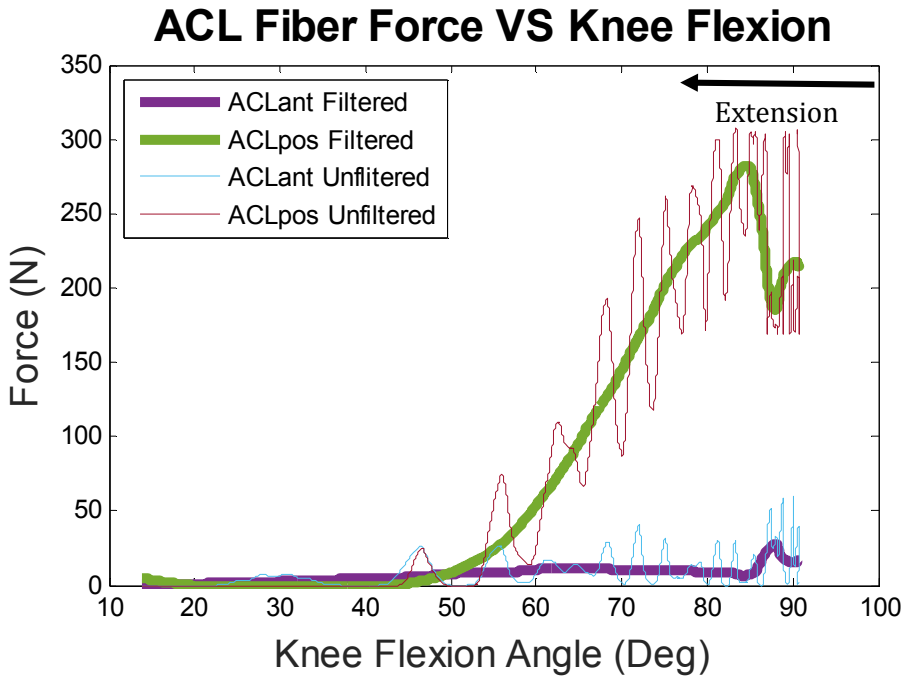

Figure 38: *ACL Fibers Forces vs Knee Flexion Angle for Knee Extension Exercise*

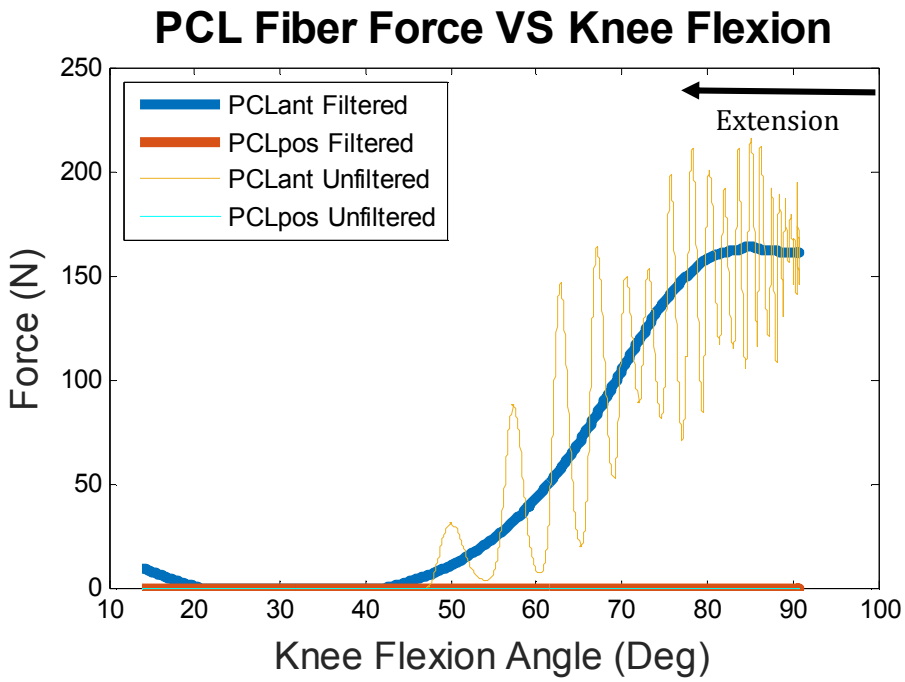

Figure 39: *PCL Fibers Forces vs Knee Flexion Angle for Knee Extension Exercise*

6.4.3 PCL Forces during Knee Extension

Unlike the ACL, the PCL forces Fig. (39) are in excellent agreement (nearly identical) with Ref. [4]. PCL anterior decreased, while PCL posterior remained zero during the extension exercise. The peak force of PCL reported in this work is 160 N while in Ref. [4] is about 120 N. It is worth noting that in Ref. (4) ligaments are not viscoelastic, but elastic.

6.4.4 Tibio-Femoral Contact Force during Knee Extension

The response of tibio-femoral contact force with respect to the knee flexion angle is similar to data reported in literature. Contact forces at 90º flexion angle (initially) are near 400N and taper down to 300N in mid flexion. The force increases at low flexion angles (close to full extension) to more than 600N. These values are in good agreement with the forces in the 3D model [4].

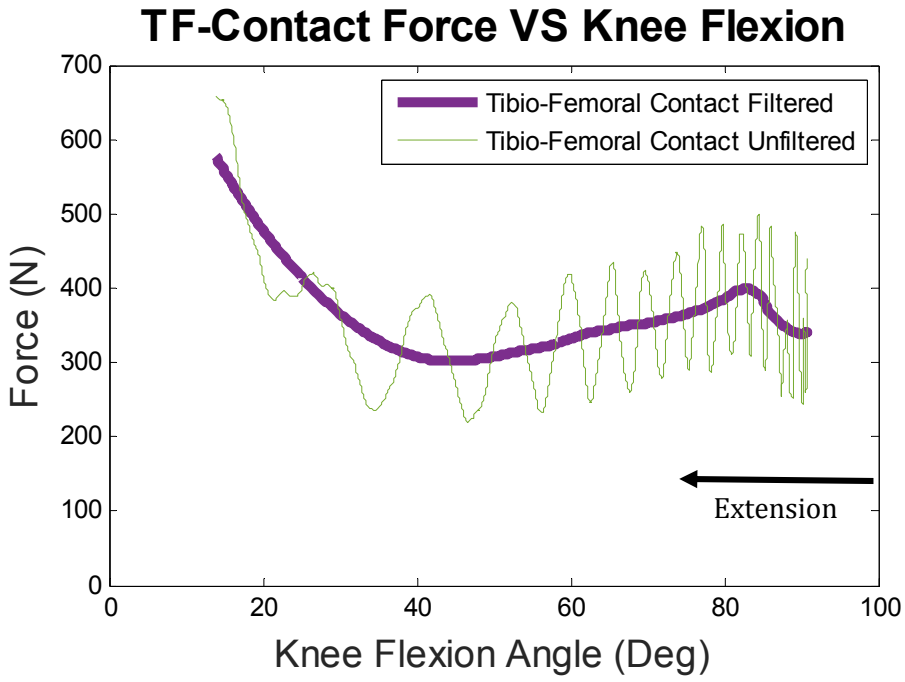

Figure 40: *Tibio-Femoral Contact vs Knee Flexion Angle for Knee Extension Exercise*

6.4.5 Patello-Femoral Contact Force During Knee Extension

In Fig. (41), the patello-femoral contact force resembles very closely (almost identical) the patella-femoral contact force found in [4] in both magnitude and pattern.

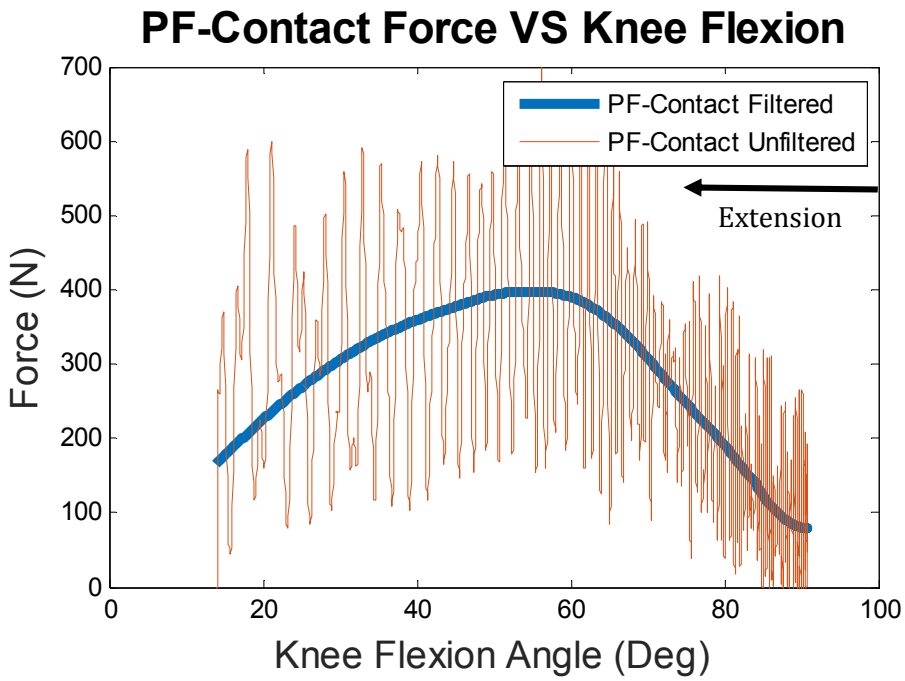

Figure 41: *Patello-Femoral Contact Force vs Knee Flexion Angle for Knee Extension Exercise*

6.5 Discussion and Conclusions

The knee extension exercise is one of the most frequently used knee exercises. It is ideal for a sagittal plane model because of the bone motions within the plane. In comparison with other models in the literature that perform knee extension, our 2D dynamic model of the human knee very closely matches other data reported in the literature. The knee model tested with *ode15s* and a DAE system of equations was able to simulate the knee extension exercise and had internal contact forces and ligament forces that were able to be validated using Caruntu and Hefzy's 3D anatomical model [4]. The 2D model uses different bone profiles, ligament characteristics, cartilage contact modeling, and makes many careful assumptions. Yet, it is still

accurate to get results that are realistic and are similar to a robust 3D model. The importance of this section was to test the knee model of this work in the case of a very common exercise, i.e. knee extension exercise. With closely resembling results during knee extension, the model is validated and it can be adapted and used for other exercises.

REFERENCES

[1] Vella, M. 2008. “Anatomy for strength and fitness training.”New Holland Publishers.

[2] Beynnon, B., Yu, J., Huston, D., Fleming, B., Johnson, r., Haugh, L., & Pope, M.H. 1996. “A sagittal plane model of the knee and cruciate ligaments with application of a sensitivity analysis.”Journal of biomechanical engineering, 118(2), 227-239.

[3] Shelburne, K.B., Pandy, M.G., 1997, “A musculoskeletal model of the knee for evaluating ligament forces during isometric contractions,” Journal of Biomechanics, Vol. 30, No. 2, pp. 163-176.

[4] Caruntu, D.I., Hefzy, M.S., 2004,” 3-D anatomically based dynamic modeling of the human knee to include tibio-femoral and patello-femoral joints,” ASME Journal of Biomechanical Engineering, Vol. 126, No. 1, pp. 44-53.

[5] Abdel-Rahman, E., Hefzy, M.S.,1993. “A two-dimensional dynamic anatomical model of the human knee joint.”ASME Journal of Biomechanical Engineering 115, 357-365.

[6] Caruntu, D., Hefzy, M.S., 2004, “The Biomechanical Function for the Patellar Tendon During In-vivio Weight-Bearing Flexion,” *Journal of Biomechanics*, 40, pp. 1716-1722.

[7] Caruntu, D., Hefzy, M.S., Goel, V.K., and et. al., 2003, “Modeling the Knee Joint in Deep Flexion: “Thigh and Calf” Contact, *2003 Summer Bioengineering Conference, June 25-29 Sonesta Beach Resort in Key Biscayne, Florida*, pp. 459-460.

[8] Hefzy, M.S., Cooke, T.D.V., 1996, "Review of Knee Models: 1996 Update", Applied Mechanics Review, Vol. 49, No. 10, part 2, pp. 1-7.

[9] Goldblatt, J. P., & Richmond, J. C. 2003. “Anatomy and biomechanics of the knee.” Operative Techniques in Sports Medicine, 11(3), 172-186.

[10] Van Dommelen, Johannes AW, et al. 2005. “Characterization of the rate-dependent mechanical properties and failure of human knee ligaments.”SAE Technical Paper No. 2005-01-0293.

[11] Haimes, J.L., Wroble, R.R., Grood, E.S., Noyes, F.R., 1994, “Role of the Medial Structures in the Intact and Anterior Cruciate Ligament-Deficient Knee: Limits of Motion in the Human Knee,” The American Journal of Sports Medicine, Vol. 22, No. 3, pp. 402-409.

[12] Sugita,T.,Amis,A.A..2001. “Anatomic and biomechanical study of the lateral collateral ligament and popliteofibular ligaments.” The American journal of sports medicine, Vol. 29, No.4.

[13] Mow, V. C., Athesian, G. A., Spilker, R. L., 1993, ‘‘Biomechanics of Diarthrodial Joints: A Review of Twenty Years of Progress,’’ J BiomechEng, Vol. 115, pp. 460–467.

[14] Zheng, N., Fleisig, G.S., Escamilla, R.F., Barrentine, S.W. 1998, "An analytical model of the knee for estimation of internal forces during exercise," Journal of Biomechanics, Vol. 31, No. 10, pp. 963-967.

[15] Abdel-Rahman, E.M., Hefzy, M.S., 1998, "Three-Dimensional Dynamic Behaviour of the Human Knee Joint Under Impact Loading," *Medical Engineering & Physics*, 20, pp. 276-290.

[16] Bendjaballah, M.Z., Shirazi-adl, A., Zukor, D.J., 1995. "Biomechanics of the human knee joint in compression: reconstruction, mesh generation and finite element analysis." Knee 2, 69-79.

[17] Li, G., Lopez, O., Rubash, H., 2001. "Variability of a three- dimensional finite element model constructed using magnetic resonance images of a knee for joint contact stress analysis." ASME Journal of Biomechanical Engineering 123, 34-346.

[18] Hefzy, M. S., & Cooke, T. D. V. 1996. "A review of knee models: 1996 update" lJ. ApplMech Rev, 49, l87-l89.

[19] Zavatsky, A. B., & O'Connor, J. J. 1992. "A Model of human knee ligaments in the sagittal plane: part 1: response to passive flexion." Proceedings of the Institution of Mechanical Engineers, Part H: Journal of Engineering in Medicine, 206(3), 125-134.

[20] Provenzano, P., Lakes, R., Keenan, T., Vanderby Jr., R., 2001, "Nonlinear ligament viscoelasticity," Annals of Biomedical Engineering, Vol. 29, pp. 908-914.

[21] Wismans, J., Veldpaus, F., Janssen, J., Huson, A., Struben, P., 1980, "A three-dimensional mathematical model of the knee-joint," J Biomechanics, Vol. 13, No. 8, pp. 677-679.

[22] Moeinzadeh, M.H., Engin, A.E., Akkas, N., 1983, "Two-dimensional dynamic modeling of human knee joint," Journal of Biomechanics, Vol. 16, No. 4, pp. 253-264.

[23] Blankevoort, L., Huiskes, R., 1991, "Ligament-Bone Interaction in a Three-Dimensional Model of the Knee," *Journal of Biomechanical Engineering*, 113 (1), pp. 263-269.

[24] Kongcharoensombat, W., Ochi, M., Abouheif, M., Adachi, N., Ohkawa, S., Kamei, G., Okuhara, A., Shibuya, H., Niimoto, T., Nakasa, T., Nakamae, A., Deie, M., 2011, "The transverse ligament as a landmark for tibial sagittal insertions of the anterior cruciate ligament: A cadaveric study, arthroscopy, Journal of Arthroscopic & Related Surgery, Vol. 27, No. 10, pp. 1395-1399.

[25] Bei, Y., Fregly, B.J., 2004, "Multibody dynamic simulation of knee contact mechanics," Medical Engineering and Physics, Vol. 26, pp. 777-789.

[26] Nisell, R., Németh, G., Ohlsén, H., 1986, "Joint forces in extension of the knee. Analysis of a mechanical model," ActaOrthopScand, Vol. 57, No. 1, pp. 41-46.

[27] Butler, D. L., Kay, M. D., & Stouffer, D. C. 1986. "Comparison of material properties in fascicle-bone units from human patellar tendon and knee ligaments."Journal of biomechanics, 19(6), 425-432.

[28] Radin, E. L., Yang, K. H., Riegger, C., Kish, V. L., & O'Connor, J. J. 1991. "Relationship between lower limb dynamics and knee joint pain."Journal of orthopaedic research, 9(3), 398-405.

[29] Küçük, H., 2006, “The effect of modeling cartilage on predicted ligament and contact forces at the knee,” Comp in Biology & Medicine, Vol. 36, No. 4, pp. 363-375.[13] Huss, R.A., Holstein, H., O’Connor, J.J., 2000, “A mathematical model of forces in the knee under isometric quadriceps contractions,” Clinical Biomechanics, Vol.15, No. 2, pp. 112-122.

[30] Richards, D. P., Ajemian, S. V., Wiley, J. P., &Zernicke, R. F. 1996. “Knee joint dynamics predict patellar tendinitis in elite volleyball players.” The American Journal of Sports Medicine, 24(5), 676-683.

[31] Quapp, K. M., & Weiss, J. A. 1998. “Material characterization of human medial collateral ligament.” Journal of biomechanical engineering, 120(6), 757-763.

[32] Pioletti, D. P. 1997. “Viscoelastic properties of soft tissues.”

[33] Provenzano, P. P., et al. 2002. "Application of nonlinear viscoelastic models to describe ligament behavior." Biomechanics and modeling in mechanobiology1.1: 45-57.

[34] Robinson, J. R., Bull, A. M., & Amis, A. A. 2005. “Structural properties of the medial collateral ligament complex of the human knee.” Journal of biomechanics, 38(5), 1067-1074.

[35] Nekouzadeh, A., Pryse, K. M., Elson, E. L., & Genin, G. M. 2007. “A simplified approach to quasi-linear viscoelastic modeling.”Journal of biomechanics, 40(14), 3070-3078.

[36] Blankevoort, L., Huiskes, R., de Lange, A., 1991, “Recruitment of knee joint ligaments”, Journal of Biomechanical Engineering, Vol. 113, No. 1, pp. 94-103.

[37] Pandy, M. G., & Sasaki, K. 1998. “A three-dimensional musculoskeletal model of the human knee joint. Part 2: analysis of ligament function.” Computer Methods in Biomechanics and Biomedical Engineering, 1(4), 265-283.

[38] Komistek, R.D., Kane, T.R., Mahfouz, M., Ochoa, J.A., Dennis, D.A., 2005, “Knee mechanics: a review of past and present techniques to determine in vivo loads,” Journal of Biomechanics, Vol. 38, pp. 215-228.

[39] Hull, M. L., Donahue, T. L. H., Rashid, M. M., & Jacobs, C. R. (2002).”A finite element model of the human knee joint for the study of tibio-femoral contact.” J BiomechEng, 124, 273-280.

[40] Amiri, S. Cooke, D. 2007. “Mechanics of the passive knee joint. Part 2: Interaction between the ligaments and the articular surfaces in guiding the joint motion.” Journal of Engineering in Medicine Vol. 221.

[41] Ateshian, G. A., L. J. Soslowsky, and V. C. Mow. 1991."Quantitation of articular surface topography and cartilage thickness in knee joints using stereophotogrammetry." Journal of biomechanics 24.8.

[42] Basso, O., Johnson, D.P., and Amis, A.A., 2001, “The Anatomy of the Patellar Tendon”, *Knee Surgery, Sports Traumatology, Arthroscopy*, 9, pp. 2-5.

[43] Blajer, W., Dziewiecki, K., Mazur, Z., 2007, “Multibody Modeling of Human Body for the Inverse Dynamics Analysis of Sagittal Plane Movements,” *Mulitbody System Dynamics*, 18, pp. 219-232.

[44] Chow, J.W., Park, S., Wight, J.T., and Tillman, M.D., 2006, "Reliability of a Technique for Determining Sagittal Knee Geometry From Lateral Knee Radiographs", *The Knee,* 13, pp. 318-323.

[45] Kuster, M.S., Wood, G.A., Stachowiak, G.W., Gächter, A., 1997, "Joint load considerations in total knee replacement," J Bone Joint Surg Br, Vol. 79, No. 1, pp. 109-13.

[46] LaPrade, R.F., Ly, T.V., Wentorf, F.A., Engebresten, L.. 2003. "A qualitative and quantitative morphologic analysis of the fibular collateral ligament, popliteus tendon, popliteofibular ligament, and lateral gastronemius tendon." The American journal of sports medicine, Vol. 31, No. 6.

[47] Messier S.P., Gutekunst D.J., Davis C., DeVita P., "Weight loss reduces knee-joint loads in overweight and obese older adults with knee osteoarthritis," Arthritis Rheum. 200 Jul; 52(7), 2026-32.

[48] Van Eijden, T.M.G.J., Kouwenhoven, E., Verburg, J., Weijs, W.A., 1986, "A mathematical model of the patellofemoral joint," Journal of Biomechanics, Vol. 19, No. 3, pp. 219-223

[49] Shepard, D. E. T., Seedhom, B. B., 1999, "The 'Instantaneous' Compressive Modulus of Human Articular Cartilage in Joints of the Lower Limb,'' Rheumatology, 38, pp. 124–132.

[50] Pandy, M.G., Shelburne, K.B., 1998, "Theoretical Analysis of Ligament and Extensor-Mechanism Function in the ACL-Deficient Knee," *Clinical Biomechanics*, 13, pp. 98-111.

[51] Shelburne, K.B., Pandy, M.G., Anderson, F.C., et. al., 2004, "Pattern of Anterior Cruciate Ligament Force in Normal Walking", *Journal of Biomechanics*, 37, pp. 797-805.

[52] Peng, X., Liu, G., Guo, Z., 2010, "Finite element contact analysis of a human sagittal knee joint," Journal of Mechanics in Medicine and Biology, Vol. 10, Issue 2, pp. 225-236.

[53] Mommersteeg, T.J.A; Blankevoort. L. 1996. "Characterization of the Mechanical Behavior of Human Knee Ligaments: A Numerical-Experimental Approach." Journal of Biomechanics Vol 29.No. 2 pg 151.160.

[54] Harner, C. D., Xerogeanes, J. W., Livesay, G. A., Carlin, G. J., Smith, B. A., Kusayama, T., ... & Woo, S. L. Y. 1995. "The human posterior cruciate ligament complex: an interdisciplinary study Ligament morphology and biomechanical evaluation." The American Journal of Sports Medicine, 23(6), 736-745.

[55] Woo, S. L. Y., Hollis, J. M., Adams, D. J., Lyon, R. M., &Takai, S. 1991." Tensile properties of the human femur-anterior cruciate ligament-tibia complex The effects of specimen age and orientation." The American journal of sports medicine, 19(3), 217-225.

BIOGRAPHICAL SKETCH

My name is Eduardo Granados and I am currently a 27-year-old graduate student who works at the Dow Chemical Company as a maintenance engineer. I enjoy long hours working on Matlab code and walks on the beach. My favorite subject has always been physics and I am very passionate about my many hobbies. I like to be up at night and go out to socialize almost every weekend. I am down for anything, and enjoy trying new things. I would like to travel the world and live in a foreign country someday. My main goal is to dunk a basketball on a regulation rim and to have a satisfying job since I will be working for at least the next 30 years.

Some of my other interests include sports, fantasy leagues, and current events. I enjoy politics and reading the news. My favorite types of movies are foreign films, and my favorite music is currently trance and alternative rock. I would like to be a DJ at some point to share my passion for music. I sincerely hope you enjoyed reading my thesis and that you learned something new. Thank you. If you would like to contact me with any questions, my future-proof email address is ezgranados@gmail.com.